FOSSIL ENERGY

DOE/BC/15108-5
(OSTI ID: 750877)

# NOVEL $CO_2$-THICKENERS FOR IMPROVED MOBILITY CONTROL

Annual Report
October 1, 1998-September 30, 1999

By
Dr. Robert M. Enick and Dr. Eric J. Beckman, University of Pittsburgh
Dr. Andrew Hamilton, Yale University

Date Published: February 2000

Work Performed Under Contract No. DE-AC26-98BC15108

University of Pittsburgh
Pittsburgh, Pennsylvania

**National Petroleum Technology Office**
**U.S. DEPARTMENT OF ENERGY**
**Tulsa, Oklahoma**

**DISCLAIMER**

This report was prepared as an account of work sponsored by an agency of the United States Government. Neither the United States Government nor any agency thereof, nor any of their employees, makes any warranty, expressed or implied, or assumes any legal liability or responsibility for the accuracy, completeness, or usefulness of any information, apparatus, product, or process disclosed, or represents that its use would not infringe privately owned rights. Reference herein to any specific commercial product, process, or service by trade name, trademark, manufacturer, or otherwise does not necessarily constitute or imply its endorsement, recommendation, or favoring by the United States Government or any agency thereof. The views and opinions of authors expressed herein do not necessarily state or reflect those of the United States Government.

This report has been reproduced directly from the best available copy.

DOE/BC/15108-5
Distribution Category UC-122

# Novel $CO_2$-Thickeners for Improved Mobility Control

By
Dr. Robert M. Enick and Dr. Eric J. Beckman, University of Pittsburgh
Dr. Andrew Hamilton, Yale University

February 2000

Work Performed Under Contract No. DE-AC26-98BC15108

Prepared for
U.S. Department of Energy
Assistant Secretary for Fossil Energy

Jerry F. Casteel, Project Manager
National Petroleum Technology Office
P.O. Box 3628
Tulsa, OK 74101

Prepared by
University of Pittsburgh
Department of Chemical & Petroleum Engineering
1249 Benedum Engineering Hall
Pittsburgh, PA 15261

Yale University
Chemistry Department
2250 Prospect Avenue
New Haven, CT 06520-8107

# Table of Contents


Executive Summary vii

1. Introduction 1
   1.1 CO2 in EOR 1
   1.2 CO2 in Well Fracturing 2
   1.3 Gelation of CO2 and Foam Generation in Dense CO2 3

2. Background 5
   2.1 Previous Research on CO2 Viscosity Enhancement 5
   2.2 Foam Generation from Carbon Dioxide 17

3. Research Objectives and Our Approach 25
   3.1 Research Objectives 25
   3.2 Research Approach 27

4. Evaluation of Semifluorinated Trialkyltin Fluoride as Direct Carbon Dioxide Thickeners 29
   4.1 Synthesis and Characterization 29
   4.2 Phase Behavior of Semifluorinated Trialkyltin Fluoride 33
   4.3 Solution Relative Viscosity Measurements 37
   4.4 Conclusions 40

5. Evaluation of Fluorinated Telechelic Disfulate as Direct Carbon Dioxide Thickeners 43
   5.1 Synthesis and Characterization 43
   5.2 Phase Behavior of Polyurethane Disulfates in Carbon Dioxide 51
   5.3 Solution Relative Viscosity Measurements 55
   5.4 Conclusions 57

6. Evaluation of Fluoroalkyl Aspartate Bisureas and Ureas for Carbon Dioxide Thickening and Microcellular Foam Generation 59
   6.1 Synthesis and Characterization 59
   6.2 Phase Behavior of Fluorinated Aspartate Bisureas and Ureas in Carbon Dioxide 66
   6.3 Viscosity Enhancement by Fluorinated Aspartate Bisureas and Ureas 73
   6.4 Microcellular Foam Generation 76
   6.5 Results and Discussion 78

7. Fluoroalkyl-Styrene Copolymers 81
   7.1 Introduction 81
   7.2 Experimental 81

7.3 Results and Discussion 84
7.4 Conclusions 91
7.5 References 93

8. Solufonated Fluoroacylate-Styrene Copolymers 107
8.1 Introduction 107
8.2 Experimental 107
8.3 Synthesis of Random Copolymers of Fluoroacrylate with Monomers Containing Acromatic Groups 110
8.4 Results and Discussion 113
8.5 References 121

Appendix. Falling Cylinder Viscometry Study 123

## Abstract

Several types of carbon dioxide thickening agents have been developed for the first time. The general classes of compounds include fluorinated polyurethane disulfides, semifluorinated trialkyltin fluorides, styrene-fluoroacrylate copolymers, sulfonated styrene-polyurethane copolymers and small, fluorinated H-bonding compounds. Each of these compounds was designed to be carbon dioxide-philic via the incorporation of fluorinated moities. Therefore these compounds do not require cosolvents to exhibit sufficient solubility in dense carbon dioxide. Further, each compound contains at least functional group that leads to the formation of macromolecules via intermolecular associations or interactions.

The most promising carbon dioxide thickener is a random copolymer of fluoroacrylate and styrene. The cloud point pressure increased from 12-17MPa as the concentration of the copolymer in carbon dioxide increased from 1-5 wt%. The solution viscosity was increased by a factor of 2-250 at concentrations of 0.2-5.0 wt% in liquid carbon dioxide. Therefore a detailed study of the viscosity of carbon dioxide-poly(fluoroacrylate-styrene) copolymers was conducted. Falling cylinder viscometry experiments were conducted over a wide range of shear rates and polymer concentrations. The solution viscosity was measured at 297 K and 34 MPa. Results demonstrated that the solution viscosity increased with polymer concentration. The solutions also exhibited shear thinning behavior, with increasing viscosity observed at lower shear rates. This viscometer could not yield data at relatively low viscosity increases (2-10 fold increase) and low shear rates

($10\text{-}20s^{-1}$) desired for EOR applications. Extrapolations of dilute solution results, however, indicated that it may be possible to increase the viscosity of dense carbon dioxide by a factor of 2-3 at low shear rates using very dilute polymer concentrations.

## Executive Summary

The objective of this contract is to design, synthesize, and characterize thickening agents for dense carbon dioxide and to evaluate their solubility and viscosity-enhancing potential in $CO_2$. Hydrocarbon-fluorocarbon random copolymers, sulfonated hydrocarbon-fluorocarbon random copolymers, semifluorinated trialkyltin fluorides, fluorinated telechelic ionomers and small hydrogen-bonding compounds have been evaluated. Random copolymers of styrene and heptadecafluorodecyl acrylate were characterized by high solubility ion dense carbon dioxide and the most substantial increases in solution viscosity. Falling cylinder viscometry results indicated that the 29%styrene-71%fluoroacrylate bulk-polymerized copolymer induced 2-250 fold increases in viscosity at copolymer concentrations of 0.2-5.0wt%.

A detailed study of the poly(fluoroacrylate-styrene) carbon dioxide thickener was completed. Close-clearance falling cylinder viscometry was used to measure solution viscosity. Aluminum cylinders of varying diameter (and therefore terminal velocity and shear rate) were used to determine the effect of shear rate on viscosity. Further, concentrations as low as 0.1wt% were tested in an attempt to identify the lowest concentration of thickener required to enhance the viscosity of dense carbon dioxide. The results indicated that the solutions were shear-thinning, and that viscosity increased with increasing concentration. The increase in viscosity attained using dilute concentrations of the thickener could not be determined with this apparatus at low shear rates (in the range

of EOR floods). Extrapolated results from higher shear rates indicated that it *may* be possible to achieve 2-fold increases in carbon dioxide viscosity using copolymer concentrations of 0.1-0.2 wt%.

These falling cylinder viscometry results serve as a screening tool for identifying compounds that completely dissolve in carbon dioxide and can significantly increase the solution viscosity. More accurate and relevant viscosity measurements will be generated in the second year of the project for promising carbon dioxide-thickeners by measuring pressure drops associated with a specified flow rate of the solution through sandstone cores. Further, we will investigate the potential of novel carbon dioxide thickeners that contain only carbon, hydrogen and oxygen. These thickeners would be substantially less expensive than fluorine-containing copolymers.

# 1. INTRODUCTION

## 1.1. $CO_2$ in Enhanced Oil Recovery

In petroleum industry, carbon dioxide can be injected into an oil field to maintain the reservoir pressure and to displace additional petroleum. This procedure is called tertiary recovery and the technique is commonly referred to as $CO_2$ miscible displacement or $CO_2$ flooding. During a miscible displacement project, $CO_2$ enters the oil bearing porous media at reservoir temperature, which is usually between 80 $^0$F and 250 $^0$F. The working pressure is adjusted to be slightly above the "minimum miscibility pressure" to ensure that the solvent strength of the $CO_2$ is great enough to obtain a high degree of solvency for the oil that it contacts. Thus, unlike water flooding in the secondary oil recovery, $CO_2$ can dynamically develop effective miscibility with petroleum and can therefore displace oil left behind by water flooding. As the reservoir fluids are produced from the production wells, carbon dioxide can be readily separated from the oil simply by pressure reduction. Other remarkable properties of $CO_2$ such as natural abundance, low cost, non-flammability, low toxicity, and classification as a non-VOC also contribute to make $CO_2$-flooding an attractive sustainable oil recovery procedure.

The foremost disadvantage of $CO_2$ as an oil displacement fluid is its low viscosity, 0.03-0.10 cp at the reservoir conditions. However, the oil to be displaced has a viscosity that varies from 0.1-50 cp, which means the viscosity of $CO_2$ can be 100

times lower than the viscosity of oil. The much lower viscosity of $CO_2$ results in its much higher mobility (defined as the ratio of fluid permeability in porous media to its viscosity) compared to oil. Thus $CO_2$ "fingers" its way towards the production well, bypassing much of the oil in the reservoir. Moreover, in stratified reservoirs, the high mobility of $CO_2$ induces it to preferentially enter highly permeable zones, leaving oil residing in less permeable layers not contacted by $CO_2$ and thus not efficiently displaced. Consequently, if the carbon dioxide viscosity could be elevated to a level comparable with the oil it is displacing, typically a 1-2 orders of magnitude increase, substantial improvement in oil recovery efficiency could result.

### 1.2. $CO_2$ in Well Fracturing

Dense carbon dioxide is also employed in petroleum industry for gas and oil well fracturing. During a well fracturing procedure, liquid $CO_2$ is delivered to the ground and cracks the well open by high pressure. Subsequently, sand particles as proppant are carried by dense $CO_2$ and sent to the crack formation to further fracture the well. The advantages of this technique, apart from the benign properties of CO2, are the elimination of residual fluid left in the formation and rapid cleanup.

The ability to enhance the viscosity of carbon dioxide could also improve the performance of this technology. An increase in viscosity could increase the fracture width by increasing the friction factor and reduce fluid leakoff. Furthermore, higher

concentrations of larger sand proppant particles can be carried by dense viscous carbon dioxide to the formation.

### 1.3. Gelation of $CO_2$ and Foam Generation in Dense $CO_2$

If we could create such molecules that would dissolve in carbon dioxide at relatively moderate pressures and then form macromolecular aggregates in solution, we could, on one hand, enhance the viscosity of $CO_2$ for the petroleum industry mentioned above. This is the primary objective of this study; the synthesis of a thickener that can result in transparent, single-phase, carbon dioxide-rich solutions that display a viscosity comparable to the oil being displaced.

On the other hand, if such aggregates formed in solution could be preserved during and *after* solvent carbon dioxide removal, a foam structure can be generated in one-step. Foamed polymeric materials have many intriguing applications ranging from thermal and electrical insulation materials, catalyst support, separation media to cell growth scaffolds in tissue engineering. Traditionally, foamed materials have been blown by chlorofluorocarbons (CFC's) due to their low boiling point and low thermal conductivity. But because of their suspected role in the deterioration of the ozone layer, replacing blowing agents such as hydrochlorofluorocarbons (HCFC's), perfluoroalkanes (HFC's) and low boiling hydrocarbons and carbon dioxide are being used. Of these replacement blowing agent, HCFC's and HFC's are very expensive and toxic; Low boiling hydrocarbons are extremely flammable. Carbon dioxide, however, has been considered to

be a much more environmental benign blowing agent because it is non-flammable, non-toxic, and naturally abundant.

# 2. BACKGROUND

## 2.1. Previous Research on $CO_2$ Viscosity Enhancement

### 2.1.1. Polymers as $CO_2$ Thickeners

Since the 1980's, several research groups have been trying to identify an effective $CO_2$ thickener which is in the first place soluble in $CO_2$ at reservoir conditions and could increase $CO_2$ viscosity by 1-2 orders of magnitude at a concentration of 1wt% or less.

The first type of thickener tested was polymers with various molecular weights. Heller and co-workers at NMIMT did extensive research on a wide range of commercially available polymers. However, due to the extremely low solubility of traditional hydrocarbon based polymers in $CO_2$, none of the polymers that they have tested came close to rendering significant viscosity increase for dense $CO_2$. From their initial test, they found that very few atactic amorphous polymers with low solubility parameters are soluble in $CO_2$ when their molecular weights go beyond 6,000. The atactic structure of the polymer was believed to maximize the entropy of mixing between $CO_2$ and polymer. They then synthesized atactic polymers of various molecular weights and with side chains of different length. Although slightly more soluble in dense $CO_2$, these polymers still did not induce a significant viscosity increase.

Terry's research group at University of Wyoming attempted to increase the viscosity of $CO_2$ via in-situ polymerization of $CO_2$-soluble monomers, hoping to form a single-

phase solution with dense $CO_2$ trapped in the polymer network. However, the hydrocarbon polymers precipitated during reaction, rather than stay in solution to render any viscosity increase. Our previous study at University of Pittsburgh with in-situ polymerization of $CO_2$-soluble fluoroether based polyurethane prepolymers (MW < 3000) also gave similar results. To obtain a single-phase polymer network with $CO_2$ dissolved in it, unrealistic amount of monomer and hence the final polymer has to be used. The final solution is actually polymer-rich instead of a $CO_2$-rich solution with a small amount of polymers dissolved in it as required for the EOR applications.

Irani and Bae at Chevron demonstrated the use of high molecular weight silicone oils to enhance $CO_2$ viscosity. Although the viscosity of $CO_2$ at 55 $^0$C and 17.2 MPa could be raised to 1.5 cp with 4wt% siloxane (MW = 197,0000), 20wt% toluene has to be used as a cosolvent, which is apparently undesirable for the field use of EOR.

### 2.1.2. Low Molecular Weight Associative Compounds as $CO_2$ Thickeners

#### 2.1.2.1. Trialkyltin Fluoride

Another series of $CO_2$ thickeners studied are relatively low molecular weight compounds that can associate in solution even at very low concentrations. The pseudo polymer networks formed through molecular association result in significant increase of solvent viscosity and even gelation.

Trinutyltin fluoride has been reported to slowly dissolve in n-hexane and cause the its viscosity to increase from 0.3 cSt to 300 cSt at a concentration of 10 g/L at 37 $^0$C. The intriguing viscosity increase results were explained on the basis of transient polymeric chain formation through intermolecular Sn-F bridging, as shown in Fig.3a. X-ray studies on crystalline trimethyltin fluoride proved that the compound exits as a penta-coordinate polymer containing Sn-F linkages. Dunn and Oldfield gave the first non-spectroscopic evidence for the existence of such pseudo polymeric chain in the solution of tributyltin fluoride in non-polar solvents by studying solvent additive effect on solution viscosity. Interestingly, the tributyltin fluoride compound is only soluble in n-hexanes, not in other alkanes.

Heller and coworkers then systematically studied the solubility behavior of various trialkyltin fluorides in Liquefied Petroleum Gas (LPG) as well as dense $CO_2$ and their capability of increasing the viscosity of the solvents used. Their findings again proved as a non-spectroscopic evidence that the large difference in the negativity of tin and fluorine atoms can indeed cause the self association of the triorganotin fluoride compounds provided that the appropriate R groups are present and the solvent is non-polar. They further found that the solubility and viscosity behavior of these compounds can be changed dramatically with very little structural manipulation. For example, by increasing the chain length of the R group from 4 to 10 the crystallinity of the compound was decreased and the overall solubility was greatly improved in most organic solvents. The trineophyltin fluoride was found to be soluble in various nonpolar solvents but unable to bring any viscosity increase because of the steric hindrance to intermolecular association

of the bulky neophyltin groups. They also introduced Si-containing groups to the trialkyltin fluoride structure trying to increase its solubility in both non-polar organic solvents and dense $CO_2$. The resultant tris(trimethylsilyl-propyl)tin fluoride instantly dissolved in normal alkanes, but the critical concentration (defined as the concentration after which viscosity increases dramatically) was above 0.7% (g/100ml) as compared to <0.5% for most of the trialkyltin fluorides. Heller and coworkers believe that this may due to some steric hindrance by the bulky trimethylsilyl groups present in the vicinity of Sn-F bond. The presumed that by pushing the Me3Si groups further away from the associative Sn-F bond, the steric hindrance could be reduced and the solution viscosity increase may be effective at lower concentrations. Despite the intriguing viscosity enhancement capability of these trialkyltin fluoride compounds in non-polar organic solvents such as hexanes and LPG, their solubility in $CO_2$ did not exceed 0.17 g/100ml and no viscosity increase could be resulted.

#### 2.1.2.2. Telechelic Ionomers

Telechelic ionomers, the polymers with relatively low molecular weights (<50,000) and with end-functionalized ionic groups, have been found to be able to gel non-polar organic solvents such as alkanes and aromatics at dilute concentrations (< 5wt%). The telechelic ionomers studied usually contains a polymeric backbone that are soluble in organic solvents and 2 or more ionic end-groups depending on the branching nature of the backbone polymer for electrostatic associations. A wide variety of polymeric backbones has been studied, including polybutadiene, hydrogenated polybutadiene, polyisobutylene,

EPDM, polystyrene, and poly(α-methyl)styrene. The associative ionic end-groups fall into mainly three categories: sulfate, sulfonate and carboxylate. Reological behavior and light scattering studies have proved that the gel and significant solution viscosity increase of telechelic ionomer in non-polar solvents are resulted from the strong dipolar interactions between the ionic end groups. For a linear difunctional chain, the ionic groups can aggregate not only into pairs and multiplets of a few ion pairs but also into clusters consist of 30-100 ion pairs, depending on the ion content. The aggregates form a supermolecular structure in solution, which is manifested as the apparent viscosity increases in solution and eventually gel formation results.

The coulombic nature of the intermolecular interactions determines that the nature of the ion pairs (valence and size), the characteristics of the polymeric backbone (MW and polydispersity), and also the polarity of the solvent all affect the association and hence the solution viscosity significantly. Many research studies with quite different telechelic ionomer-solvent systems have shown that ion pairs with higher valence and smaller size have stronger intermolecular interactions. The lower the PDI of polymeric backbone, the sharper the viscosity change versus concentration. At low molecular weight range, which is usually below 20,000, ionic concentration is more important than the molecular weight because the ionic interaction dominates. As the molecular weight of the backbone increases, the ionic concentration decrease accordingly, thus leading to gel at higher concentrations. When the molecular weight is much higher, there should be a point when chain entanglement contributes more to the network formation than the ionic interactions,

resulting in a decrease of the gelation concentration as molecular weight increases. The electrostatic interactions in non-polar solvents can be easily disrupted by the addition of more polar solvents such as alcohol, THF, DMF, et. al., leading to much higher concentration of gelation or no gelation at all at the low concentration range.

Heller at NMIMT also studied the possibility of using hydrocarbon-based telechelic ionomer as an effective thickener for dense $CO_2$ in his evaluation of sulfonated polyisobutylene. The result, as can be predicted, is that this ionomer exhibit vanishingly low solubility in $CO_2$, leading to no viscosity increase at all. Because of the poor solvent power of dense $CO_2$, hydrocarbon-based unfunctionalized polymers are essentially insoluble in $CO_2$, and the addition of ionic end groups further reduces the solubility of these telechelic ionomers.

#### 2.1.2.3. Low Molecular Weight Hydrogen Bonding Compounds

In recent years, a number of low molecular weight organic compounds have been designed to self-assemble in solid state and in solution through weak non-covalent interactions to render intriguing properties. In organic solvent solution, these compounds self-assemble through highly specific interactions into elongated fiber-like structures. These fibers in turn form a three-dimensional network encapsulating the solvent, thus form a gel. The well-defined open network structures offer new possibilities of developing functional gels that are useful in area such as catalysis, sensor technology and material science by incorporating recognition sites into the network molecular structure. The most

remarkable characteristics of these organic compounds is that they are very effective gelling agents, with a gelling concentration of approximately 1wt%. Compounds with compact hydrogen bonding center cores such as cyclohexane and benzene form one-dimensional linear hydrogen bonding aggregates, the aggregates can then further associate through interdigitation of the side chains to form networks in solution. Compounds with extended chains between hydrogen bonding groups form two-dimensional sheet structure aggregates, which in turn can be associated with other sheet aggregates by Van der Waals interactions between the long side chains.

The general structure of these compounds consists of at least one hydrogen bonding functionality such as urethane, amide, or urea. Although most gel network are formed by incorporating 2 or three hydrogen bonding functionalities, Hanabusa and co-workers have successfully gelled a variety of organic solvents with *N*-benzyloxycarbonyl-L-alanine 4-hexadecanoyl-2-nitrophenyl ester, which has only one urethane hydrogen bonding functionlity. The arrangement of the hydrogen bonding groups can also be quite different. For instance, they could be located at the equatorial positions of the cyclohexane or benzene ring, they could also be located adjacent to each other around the ring structure, or they could even be at each end of a short linear chain.

Also responsible for the three dimensional network formation is the existence of other organic moieties in the molecular structure to provide weaker and less specific intermolecular interactions through $\pi$-$\pi$ stacking and/or Van der Waals interactions

between long side chains sticking out form the hydrogen bonding center core. Basically, the successful formation of such gels or viscous liquid in organic solution depends on the nature of both the solvent and the gelling agent. With slightly changed structures, this type of compound can gel almost any organic solvent from the more polar solvent like methanol and acetone, to the almost non-polar solvent like benzene and hexanes. Hamilton and Hanabusa both found that the appropriate type and length of the side chains are essential to dissolve the compound in organic solvents and to prevent the transformation of gels/viscous solution into crystals. Hamilton's research group has found that the simple tris-analide of cyclohexane-1,3,5-tricarboxylic acid was insoluble in all organic solvents. However, the corresponding 6-picoline derivative readily dissolved in chlorocarbons. Hanabusa and co-workers studied the viscoelastic behavior of organic solvents containing trialkyl-1,3,5-benzenetricarboxamides with different side chain lengths and found that side chains of sufficient length/carbon numbers (8 is the critical carbon number in their research) are required to result in the solubility and against crystallization. Although not necessary, the existence of aromatic structures in the molecules contributes both to the intermolecular association through $\pi$-$\pi$ stacking and to the solubility of the compounds by providing interactions with the solvents.

The solubility and viscosity enhancing capability of these hydrocarbon-based hydrogen bonding associative compounds were never tested in dense $CO_2$. However, based on the much poorer solvent power of dense $CO_2$ compared with hydrocarbon solvents, we could predict that these compounds with hydrocarbon side chains and strong

polar groups such as amide and urea cannot easily dissolve in $CO_2$ to render any significant viscosity increase.

#### 2.1.2.4. Other low molecular weight associative compounds

Apart from the low molecular associative compounds mentioned above, several other low molecular weight compounds are discovered to be able to gel organic solvents and therefore tested in carbon dioxide.

One of the compounds is traditional water soluble surfactants with unique molecular structures. Viscoelastic networks or gels can be formed in organic solvents at surfactant concentration as low as 1wt% with the existence of a small amount of water (up to 5wt%) in the system. Hoffmann reviewed this type of fascinating phenomena exhibited by surfactant systems and concluded that the shape of the micelles basically determines the possibility of the three-dimensional network/gel formation. Micelles with rod-shaped packing can entangle with other micelle aggregates, forming an infinite network. Such network can be further swollen without damage to some extent by adding hydrocarbon solvents. Microscopically, the shape of the micelles in turn is controlled by the packing parameters of the surfactant molecules in the aggregate assembly. If the cross-sectional area of the head group $a_h$ is larger than that of the chain $a_c$ in a surfactant molecule in its average surrounding, the system will form micellar aggregates with a convex curvature. If $a_h < a_c$ , the system prefers to form an inverse structure. When both areas are of the same size, planar packing structures are favored and a rod-shaped aggregate is formed.

The surfactant used could be either ionic or nonionic. For example, fluorinated alkyldimethylamine oxide has been observed to gel fluorinated liquid at very low concentrations (below 1wt%).

Surfactants with high valence bulky counter ions such as aluminum, zinc are proved to be very effective gelling agent for organic solvents like alkanes. These surfactants are able to former dimers through the high valence counter-ion providing additional strong association between molecules. In effect, a concentration as slow as 0.75wt% of aluminum alkanoate was needed to gel gasoline.

12-Hydroxyoctadecanoic acid (or hydroxystearic acid), though not a surfactant, has been found to exhibit similar gelling behavior to that mentioned above. Due to the intermolecular hydrogen bonding and the existence of chiral carbon in its molecules, it could form supramolecular helicoidal structures in $CCl_4$ and some aromatic solvent and gel these organic solvents.

Previous research in our group has evaluated surfactants such as aluminum disoap and fluoroalkyl amine oxide as $CO_2$ thickeners. However, the compounds either do not dissolve in carbon dioxide or fail to form favorable rod-like aggregates that leads to gel formation. Heller's research group evaluated 12-hydroxylstearic acid as $CO_2$ thickeners and concluded that a significant amount of cosolvent, such as 10-15% ethanol has to be used to result in its solubilization in $CO_2$ to form a gel.

### 2.1.3. $CO_2$-philic Functionalities

The apparent obstacle to transform the effective organic solvent gelators into successful dense $CO_2$ thickeners is the insolubility of these compounds in $CO_2$. To increase the thickener solubility and hence $CO_2$ solution viscosity, prohibitively large amount of organic co-solvents have been reported to be used to bring the compounds into solution. However, from both economic and environmental point of view, a direct $CO_2$ thickener is required, or rather, the co-solvent effect should be from the molecular structure of the functional thickener itself.

In the last decade, much research has been done on identifying $CO_2$-soluble molecular structures, hereafter called $CO_2$-philic functionalities, and the mechanism of the solubility of certain molecules in dense $CO_2$. One widely accepted general rule to predict the miscibility of fluids is that fluids are thought to have a high probability of being miscible if their solubility parameters are comparable. Calculation from an equation of state suggest that the solubility parameter of $CO_2$ approaches that of normal alkanes above 30 MPa, hence, for many years, the solvating power of $CO_2$ was thought to be like that of hexanes. However, the insolubility of most hydrocarbon-based compounds and polymers in dense $CO_2$ led researchers to find more strict and extensive standards to describe the intriguing solvent power of $CO_2$. Among them, Johnston and collegues have suggested that CO2's quadrupole moment tends to inflate the calculated solubility parameter by almost 20%, indicating that the true solubility parameter of carbon dioxide is more like

that of silicones or fluorinated compounds. Recent work by Beckman's group and DeSimone's group has shown experimentally that high molecular weight silicones, fluoroalkyls, fluoroethers and fluoroacrylates are miscible with carbon dioxide at moderate pressures, while conventional alkyl functional polymers and oligomers are nearly insoluble. The molecular structures of these CO2-philic functionalities are shown in Fig. 7a-d. Among these $CO_2$-philic functionalities, fluoroethers, for example, have the lowest solubility parameter of any conventional liquid and exhibit extremely high carbon dioxide solubility.

Solubility parameters alone, however, are not sufficient to explain and predict the solubility of a certain compound in carbon dioxide. The Lewis acid nature of carbon dioxide makes one to speculate that $CO_2$ would exhibit specific interactions with Lewis bases. This explains quite well the solubility of polypropylene oxide and polyethylene oxide oligomers in $CO_2$ at moderate pressures if we could envision favorable acid-base interactions between the electron-rich ether groups in the polymers and the electron-poor carbon of $CO_2$. Further, fluorinated alkanes and liquid carbon dioxide are found to be the only type of compounds that exhibit negative dipolarity/polarizability parameters, $\pi^*$. The experimental results of Yee and coworkers led them to speculate that repulsion between fluorinated compounds was responsible for their high solubility in carbon dioxide.

Although the exact mechanism responsible for the enhanced solubility of fluorinated and silicon based compounds in carbon dioxide have not been identified,

experimental results from several research groups have shown that the incorporation of $CO_2$-philic functionalities into the structures of surfactants, dispersants, and chelating agents has greatly enhanced their $CO_2$ solubility, making it possible to use $CO_2$ for polymerization, metal extraction, foam generation and other more sustainable processes.

In their research for $CO_2$ soluble polymers, DeSimone and coworkers observed that poly(1,1-dihydroperfluorooctyl acrylate) (PFOA, estimated MW = $1.4 \times 10^6$) can be solution polymerized in supercritical $CO_2$ and remain soluble after polymerization without the need for a cosolvent. The corresponding viscosity changes of the polymer-$CO_2$ solution up to several weight percent were also documented. With a polymer concentration of 5-10wt%, this high molecular weight random coil polymer could raise the viscosity of carbon dioxide by 3-8 fold at 50 $^0$C and a pressure range of 200-350 bar.

During our previous research to identify $CO_2$ soluble functionalities, we also investigated the viscosity enhancing ability of fluoroethers with molecular weight as high as 30,000. Although these polymers exhibited remarkable $CO_2$ solubility, with a miscible pressure (cloud point pressure) as low as 13.8 MPa, the induced viscosity increase is marginal in dilute concentrations.

## 2.2. Foam Generation from Carbon Dioxide

### 2.2.1. Foam production methods and structure characterization

Commercial low density rigid and flexible foams have been produced continuously. In these processes, a blowing agent is mixed physically with polymer melt or polymer precursor materials in an extruder or generated through polymerization reactions. At the appropriate stage of the hardening of melt and curing of reaction mixtures, pressure is released, and foamed materials are generated. Typically, the amount of blowing agent in the polymer matrix is lower than 5wt%. These processes can produce foam with greater than 95% density reduction compared to the parent polymer, but cell sizes are usually rather large, often 1mm in diameter.

The performance of the generated foam materials depends on the properties such as bulk density, open/closed cell type, cell size and orientation.

(1) Bulk Density

The bulk density of the foamed materials is the mass of parent polymer divided by the total volume after the foaming process. Here the mass of the blowing agent or air is not taken into account because of their much lower density compared to the polymer blown. The resulted foam bulk density is related to not only the conditions of the foaming process, for instances, the amount of blowing agent mixed with the melt, process temperature and pressure, but also the polymer matrix property like the density and viscosity of the parent polymer.

The foam bulk density is critical to the insulating performance of a rigid foam. The blowing agent is typically a much better insulator than the solid polymer, with the

conductivity of polymer 10-20 times greater than the conductivity of the gas. Thus higher density indicates higher polymer to blowing agent ratio, and the conductivity of the polymer predominates, which in turn decreases the insulating performance of the foam.

(2) Cell Type, Size and Orientation

Open or closed cell structure is the result of the parent polymer property and the type of blowing agent used. Foams with closed cell structures are composed of isolated closed cavities in the polymer matrix with cell walls remain intact during foam formation. If the cell walls are destroyed during the foaming process, an open cell structure with connected cell cavities will result. In some cases, the cell walls reduce to strutlike structure, leaving a reticulate foam morphology.

Closed cell rigid foams have very low thermal conductivity coefficients and are excellent insulating materials. Open cell flexible foams, however, have better sound absorption properties.

Cell size or cell diameter is another important property that determines the application and performance of the final foam product. Due to the quite different mechanism for cell formation and growth in a single piece of foam material, there exists a distribution for cell sizes. Sometimes, even a bimodal distribution can result when cell sizes of different range coexist. As insulation materials, foams with smaller cell diameters have improved

insulation efficiency because of less heat loss due to radiation and conduction. When specially foamed materials are used as membrane separation media, however, cell size directly controls the separation effectiveness and efficiency.

Foams with spherical cells are isotropic, with the same properties in all directions. If cells are elongated in the direction of rise, the cells will have ellipsoidal shapes and render the foamed materials with anisotropic properties. Isotropic foam structure can be generated when foam is allowed to form slowly and uniformly. Anisotropic foam results when foam cells grow rapidly through narrow cross-sectional area. For anisotropic foams, Averages of the properties both parallel and perpendicular to the foam rise direction are necessary to characterize the foam.

### 2.2.2. Foam Generation from Dense $CO_2$

#### 2.2.2.1. The possibility and advantages of using SCF $CO_2$ for foam generation

A fluid is said to be in its supercritical state when the temperature and pressure exceed its critical temperature and critical pressure. The critical temperature for carbon dioxide is 31.1 $^0$C, and the critical pressure is 73.8 bar. Above this temperature and pressure, carbon dioxide, like any other supercritical fluid, act as both a liquid and a gas, that is, it has the solvent characteristics of a liquid, but it can be compressed and have the diffusion characteristics of a gas.

In the supercritical state, carbon dioxide is said to be in a single fluid phase, which does not have a vapor-liquid equilibrium. Therefore, it has one more degree of freedom than vapor-liquid equilibrium system. As far as solvent power is concerned, the temperature of a liquid can be changed or a mixture of solvents can be used to adjust solvent power. For a supercritical fluid, its solvent power generally increases as a function of increasing density. As a result, the solvent power of supercritical carbon dioxide can be easily adjusted simply by changing the operating temperature and pressure, which in turn affects the density of supercritical carbon dioxide.

Supercritical carbon dioxide has been observed to swell and significantly plasticise many amorphous polymers such as poly(methyl methacrylate), polystyrene, polycarbonate, and poly(ethylene terephthalate), and subsequently depress their glass transition temperature sometimes to near room temperature. For example, the $T_g$ of polystyrene is depressed by $CO_2$ from normal value of 85-125 $^0$C to 30-40 $^0$C at 200 atm of pressure. This remarkable plasticization effect makes polymer processing and foam generation possible at lower and even ambient temperatures.

#### 2.2.2.2. Mechanisms of foam generation in SCF $CO_2$

The three most widely used methods to generate foams from supercritical $CO_2$ are: gas expansion, pressure quench, and phase separation. For the gas expansion method, a polymer sample is saturated with $CO_2$ at room temperature and foamed by gas expansion due to temperature rise above the normal $T_g$. In a pressure quench induced foam

generation, supercritical $CO_2$ at high a pressure of up to 35 MPa and a temperature higher than the critical temperature is used to swell the polymer sample and lower its $T_g$ to a point below the operating temperature. A rapid pressure quench leads to the formation of pores, while diffusion of $CO_2$ from the swollen polymer matrix into pores and out of the sample eventually raises the $T_g$ until the sample vitrifies. A pressure quench from supercritical conditions at constant temperature ensures that no vapor-liquid boundary is encountered which can damage the cellular structure of a foam.

Lastly, cellular foam structure can be generated by chemical reaction and/or crosslinking induced phase separation from SCF $CO_2$ solution. In this technique, polymerization/network formation and foam generation can be accomplished in a single vessel. Initially, the precursors are miscible with $CO_2$ above certain threshold pressures to give an initial homogeneous solution. Reactions can be conducted below or above the critical temperature of $CO_2$ as required by the natures of the reactions. As the reaction proceeds, molecular weight increases and/or network forms which makes phase separation to occur even before the reaction is completed. In this case, pores can be generated during the reaction stage and also during the ultimate pressure drop when $CO_2$ is removed, which could lead to broader cell size distribution. When time allowed for the reaction to proceed until the polymer network has been sufficiently crosslinked and then vitrified, smaller cells may be produced because of the high resistance of the polymer matrix to cell growth.

#### 2.2.2.3. Operation conditions and foam morphology

When supercritical $CO_2$ is used to generate foam from a given parent polymer matrix, both operation temperature and pressure can be changed to give the final foamed materials quite different morphologies.

Most techniques that use carbon dioxide as the foam generation fluid takes advantage of the $T_g$ depression effect of the polymer substrate by supercritical $CO_2$. So the temperature at which the substrate is foamed significantly affects the foam morphology. In a study of microcellular polystyrene foam generation from supercritical carbon dioxide, McCarthy and coworkers found that higher temperature led to larger cell sizes and lower foam bulk density. For example, the cell size increases from 1 μm at 40 $^0$C almost exponentially to 27 μm at 120 $^0$C in an unconstrained vessel, while the bulk density drops linearly from 0.82 at 40 $^0$C to 0.05 at 120 $^0$C. Higher temperature indicates lower CO2 density at the same pressure, which leads to lower swelling of polymer substrate by $CO_2$ and hence fewer nuclei generated. On the other hand, increasing temperature enhances $CO_2$ diffusion and reduces substrate viscosity, allowing cell to grow to larger sizes before the substrate vitrifies. Therefore, at higher temperature, highly expanded foams with low density and larger cells can be obtained as long as there is no volume constraints.

Parks and Beckman studied the polyurethane foam formation in supercritical carbon dioxide by carrying out polymerization in $CO_2$ and subsequently removing $CO_2$ via depressurization. In one set of experiment, a blend of polypropylene oxide diol monomer and a tetraol crosslinker (80:20 mol ratio) was reacted with TDI to form a

polyurethane network in carbon dioxide at a pressure of 21 MPa and at various temperatures. They found the cell sizes in the foam generated after CO2 removed follow a reverse trend to that found by McCarthy and coworkers, that is, the higher the reaction and saturation temperature, the smaller the cell sizes. They speculate that the lower CO2 density at higher temperature reduces the solvent power of $CO_2$ for the crosslinked polymer network. Therefore, at higher temperatures, the reaction may cause phase separations and the polymer network provide greater resistance to cell growth, leading to smaller cell sizes.

Pressure is another important variable that affects the final morphology for foams processed in supercritical carbon dioxide. In this aspect, the saturation pressure, the depressurization rate and also depressurization profile all could be adjusted to give foams with significantly unique microstructures. Generally, higher pressure means greater supersaturation upon pressure release and leads to more nucleation sites in the polymer substrates, hence smaller cell size when pressure is rapidly removed. Researches in several groups on different polymeric foams from supercritical carbon dioxide have found similar trend. By increasing reaction/saturation pressure, foams with honeycomb structure and smaller cell sizes are usually obtained, but the bulk density are usually higher than foams with larger cells due to the existence of thick cell walls. When allowed to develop by slow depressurization, cells can grow to larger sizes. However, in this case, coalescence may also occur, leading to a leveled off bulk density as found by McCarthy and coworkers. By depressurizing in two stages, nucleation at different pressure drop stages may occur and cells can subsequently grow into a bimodal foam morphology.

# 3. RESEARCH OBJECTIVES AND OUR APPROACH

## 3.1. Research Objectives

### 3.1.1 Thickening Carbon Dioxide

Due to poor solvent power of dense carbon dioxide, traditional hydrocarbon based polymers and low molecular weight organic solvent thickeners failed to dissolve in it and induce any significant viscosity increase. Our goal is to design the structure of direct $CO_2$ thickeners in such a way that the solubility enhancing structure is incorporated into the molecular structure itself, and the molecules are able to dissolve in carbon dioxide under relatively moderate pressures without the need of any additional cosolvents. In other words, we will modify the thickener structures by replacing the hydrocarbon backbone with $CO_2$-philic functionalities such as fluoroether, fluoroalkyl and fluoroacrylate to impart relatively high carbon dioxide solubility to the compounds.

On the other hand, we found that very high molecular weight $CO_2$-soluble random coil polymers are not efficient $CO_2$ thickeners. As indicated by Mark-Houwink's equation, solution viscosity and polymer molecular weight are related by a power law. Therefore the polymer molecular weight must be extremely high or even go to infinity if we want a gelled solution. The synthesis of such extremely high molecular weight polymer is not easy and its solubility in dense carbon dioxide can still be a problem even if they have the $CO_2$-philic functionalities in their structures because molecular weight is also important to determine the solubility of polymer in carbon dioxide. When the molecular weight is very high, a polymer made of $CO_2$-philic functionalities will become less soluble due to the

unfavorable entropy of mixing. With the readily achievable molecular weight (up to $1x10^6$), the concentration of a $CO_2$ soluble polymer has to be very high to obtain a significant solution viscosity.

For this reason, instead of using ultra-high molecular weight polymer, we choose to take advantage of the association between low molecular weight compounds, which are successful organic solvent thickeners. We will incorporate $CO_2$-philic functionalities into the structures of trialkyltin fluoride, telechelic ionomers, and compounds that can associate to form a network in organic solvent via hydrogen bonding to make them dissolve in dense carbon dioxide, then associate through non-covalent intermolecaular interactions to create a thermodynamic illusion of very high molecular weight. We will also copolymerize a $CO_2$-philic monomer with a monomer that has hydrogen bonding sites in its structure, trying to impart both high solubility and greater interactions among polymer chains.

### 3.1.2 Forming High Porosity, Microcellular Foams

We will further investigate the possibility of generating freestanding foams from networks in dense carbon dioxide after $CO_2$ removal. *Note that these foams are rigid foams of high porosity and microcellular structure. They can be made from the same types of materials used to form viscous carbon dioxide-rich solutions simply by cooling the solution to ambient temperature and removing the carbon dioxide.* Much research has shown that molecules can be designed to aggregate in solution via non-covalent

intermolecular associations, only rarely can these network structures be preserved after solvent removal. By tuning the molecular structure of the associative compound and adjusting the initial solution conditions such as concentration, temperature, and pressure, we could induce a phase separation by network formation, and subsequently produce microcellular materials via depressurization. Such micorcellular materials are organic analogue to the silica aerogel, but can be produced from a carbon dioxide solution in one-step without the use of large amount of anti-solvents to induce a phase inversion.

### 3.2. Research Approach

Based on the above guidelines, we will:

(1) Synthesize trialkyltin fluorides with different fluorinated carbons at every chain end and evaluate their solubility in carbon dioxide. Solution viscosity at low concentrations (up to 5wt%) will be measured by falling cylinder viscometer in a high pressure windowed cell. Ch. 4.

(2) Synthesize a relatively low molecular weight telechelic disulfate from a fluoroether diol. Molecular weight of the telechelic disulfate can be changed by extending the diol with diisocyanates to give a mostly fluorinated carbon dioxide soluble polyurethane backbone. The solubility of disulfates in $CO_2$ will be tested by cloud point pressure measurement. Their solution viscosity enhancing ability will be evaluated and compared with a high molecular weight $CO_2$ soluble polymer. Ch. 5.

(3) Synthesize $CO_2$ soluble analogue of small molecules that have hydrogen bonding points in their structure by reacting a fluoroalkyl or fluoroether alcohol with *N*-

protected asparatic acid, followed by a reaction with diisocyanates, isocyanates to incorporate hydrogen bonding moities into compound structures. Their solubility in dense $CO_2$ will be evaluated and solution viscosity be measured. Microcellular material generation in $CO_2$ with the synthesized hydrogen bonding compounds will be investigated and conditions like compound structure, concentration, and so on that determine the formation of such material and affect foam structures will be carefully studied and discussed. Ch. 6.

(4) Copolymers of a fluorinated acrylate and styrene were synthesized to enhance the viscosity of liquid carbon dioxide. The fluoroacrylate functionality imparted carbon dioxide solubility, while the styrene functionality enabled intermolecular – bonding of the aromatic groups to occur. Ch. 7 and Appendix.

(5) Sulfonate-functionalized fluoroacrylate-styrene random copolymers will be evaluated to determine if substantial increases in intermolecular associations, and hence viscosity, can be achieved without significantly diminishing the carbon dioxide solubility of the polymer. Ch. 8.

# 4. EVALUATION OF SEMIFLUORINATED TRIALKYLTIN FLUORIDE AS DIRECT CARBON DIOXIDE THICKENERS

## 4.1. Synthesis and Characterization

### 4.1.1. Materials

2-perfluoro-1-iodoethane and 1-iodo-4,4,4-trifluorobutane were purchased from Lancaster Synthesis Inc and used as received; Magnesium powder, ~50 mesh and phenyltintrichloride was obtained from Aldrich and used as received. Diethyl ether was distilled over sodium-hydroquinone. Argon was obtained from Praxair and passed through a $CaCl_2$ drying tube before use. All other reagents and solvents were purchased from Aldrich and used without further purification.

### 4.1.2. Reactions

The synthesis of tris(2-perfluorobutyl ethyl)tin fluoride and tris(3-perfluoromethyl propyl)tin fluoride were carried out with the kind help Dr. Curren's group of the Chemistry Department at the University of Pittsburgh. The reaction scheme is as follows, with the synthesis of tris(2-perfluorobutyl ethyl)tin fluoride shown below as an example. The synthesis of tris(3-perfluoromethyl propyl)tin fluoride was done similarly with only the iodo-precursor changed from 2-perfluoro-1-iodoethane to 1-iodo-4,4,4-trifluorobutane.

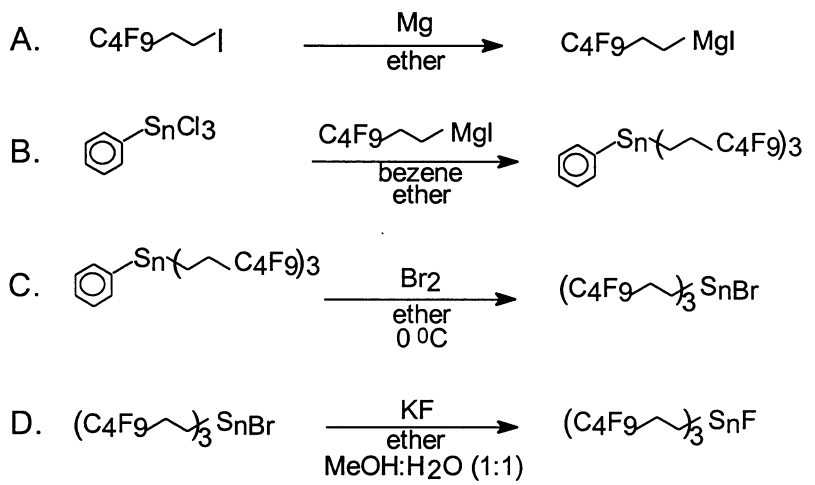


Fig.1. Reaction scheme for the preparation of semifluorinated trialkyltin fluoride

### 4.1.3. Procedure

(1) Preparation of Grignard Reagents

A 500ml three-neck flask, a stirring bar, and a reflux condenser were dried in an oven overnight and then cooled under argon. Dry ether (20ml) and 2-perfluorobutyl-1-iodoethane (1ml) was added to magnesium powder (2.91g, 120mmol) in the dried flask equipped with a reflux condenser, a thermometer, and an outlet to argon. The reaction was initiated with sonication for thirty minutes. Additional dry ether (70ml was added to the mixture while stirring. In a separate 100ml round bottom flask cooled with argon, dry ether (45ml) was combined with 2-perfluorobutyl-1-iodoethane (13.70ml, total of 60mmol). This separate mixture was slowly added to the reaction mixture over a one hour time span while stirring. The addition rate was minitored by keeping a constant

temperature of 30 $^0$C. The reaction mixture was refluxed for two and a half hours in an oil bath at 50 $^0$C and allowed to stand until it reached room temperature.

(2) Preparation of Tris(2-perfluorobutyl ethyl)phenyltin

Phenyltintrichloride (2.46ml, 15mmol) was dissolved in dry benzene (30ml) in a 100ml round bottom flask under argon at room temperature. This solution was then slowly added to the 500ml three-neck flask containing the Grignard reagent at toom temperature over a one hour time sapn while stirring. The addition rate was monitored by keeping a constant temperature of 25 $^0$C. The reaction mixture was refluxed overnight in an oil bath at 50 $^0$C and allowed to stand for four and a half hours with stirring. The reaction mixtures was diluted with ether (100ml). The mixture was then vacuum filtered into a 1L Erlenmeyer flask and hydrolyzed with saturated ammonium chloride solution (300ml). Excess magnesium solid was also hydrolyzed with saturated ammonium chloride (100ml) separately and discarded. The mixture was transferred to a 1L separatory funnel. The organic layer was dried with dried over magnesium sulfate and filtered under vacuum and the excess solvent was evaporated to dryness under reduced pressure using a rotovap. The crude product was redissolved in ether 920ml) and transferred to a 50ml flask. The ether was evaporated off under reduced pressure. Dimer impurity was removed by vacuum distillation at 0.02 torr, 100-120 $^0$C for 5 hours. The residue was further purified by passing through a silica column under pressure with hexanes as the eluent. Solvent was then removed under reduced pressure, leaving a colorless oil product, 17.2g, 93% yield.

(3) Preparation of Tris(2-perfluorobutyl ethyl)tin bromide

The obtained tris(2-perfluorobutyl ethyl)phenyltin (17.2g, 13.9mmol0 and dry ether (80ml) were transferred to a 250ml three-neck flask that was dried in an oven and cooled down to 0 $^0$C under argon. Bromine (0.71ml, 14mmol) was added dropwise to the mixture. The addition rate was monitored by keeping the temperature between 0-1 $^0$C and the addition took approximately thirty minutes. The mixture was warmed to 25 $^0$C over seven hours while stirring. The reaction mixture was transferred to a 250ml round bottom flask. The ether and excess bromine were removed under reduced pressure. The obtained oil layer was then dissolved in FC-72 (3M fluorinated solvent, 75ml) and transferred to a 250ml separatory funnel. The bromine and bromobenzene byproducts were removed by washing with methylene chloride three times (3 x 75ml). The residual solvent was removed under reduced pressure leaving 15.8g colorless oil, 92% yield.

(4) Preparation of Tris(2-perfluorobutyl ethyl)tin fluoride

500mg of tris(2-perfluorobutyl ethyl)tin bromide (0.532mmol) was dissolved in 5ml ether. To the solution was added a solution of 250mg of KF (5.95mmol) in 2ml methanol water mixture (1:1 v/v). The reaction mixture was stirred at room temperature overnight. Evaporate ether and methanol under reduced pressure. The product was then re-dissolved in 5ml ether and washed with 10ml water twice to remove excessive KF. The ether layer was then dried over magnesium sulfate and solvent removed until dryness. A clear viscous oil product layer was obtained.

(5) Preparation of Tris(3-perfluoromethyl propyl)tin fluoride

The preparation of tris(3-perfluoromethyl propyl)tin fluoride followed the similar procedure. After reaction with KF, the solvents were removed and revealed a solid crude product. This crude product was then washed with water 10ml twice and dried under vacuum until dryness.

### 4.1.4. Characterization

$^1$H NMR obtained with a Bruker MSL 300 nuclear magnetic resonance spectrometer for the product tris(2-perfluorobutyl ethyl)tin fluoride showed methylene proton at 2.58 ppm ($C_4F_9CH_2CH_2$), and also methylene proton at 1.45 ppm ($C_4F_9CH_2CH_2$). NMR spectra are shown in Appendix A.

## 4.2. Phase Behavior of Semifluorinated Trialkyltin Fluoride

### 4.2.1. Experimental Set-up

The phase behavior and viscosity measurements were performed at room temeprature using a high pressure, variable-volume, windowed cell, with a cylindrical sample volume, schematically shown in Fig.2. The system is rated to 180 $^0$C and 70 MPa.

Isothermal compressions and expansions of mixtures of specified overall composition were used to determine the two-phase boundary. A specified amount of the

sample was introduced to the sample chamber, together with several stainless steel mixing beads. High pressure carbon dioxide was then injected from a positive displacement pump into the sample volume at the same volumetric flow rate as the overburden fluid was being withdrawn, thereby expanding the sample volume. This resulted in a well-controlled, isothermal, isobaric addition of a specified amount of high pressure, liquid carbon dioxide into the sample volume.

The sample volume was then isolated and the pressure of the sample volume increased to 40 MPa. The entire view-cell was then rocked until the sample had dissolved, yielding a transparent, single-phase solution. The pressure of the sample volume was then slowly reduced by withdrawing the overburden fluid and expanding the sample volume. The pressure was reduced until visual observations of the initial appearance of a second phase occurred. The pressure was subsequently increased again and the cell rocked until the sample re-dissolved in carbon dioxide. The expansion was then repeated at a slower volumetric rate and the cloud point (dew point) pressure determined. This procedure was repeated several times and an average cloud point pressure was recorded. The cloud point pressure is the minimum pressure at which the sample is miscible with dense carbon dioxide at that particular temperature and overall composition. Below this pressure, the system consists of a sample-rich phase and a carbon dioxide-rich phase. Thus in this way we could obtain a point on the two-phase boundary of a P-x diagram. A series of these experiments was conducted over a range of overall compositions, enabling the two-phase boundary of the carbon dioxide-thickener system to be established.

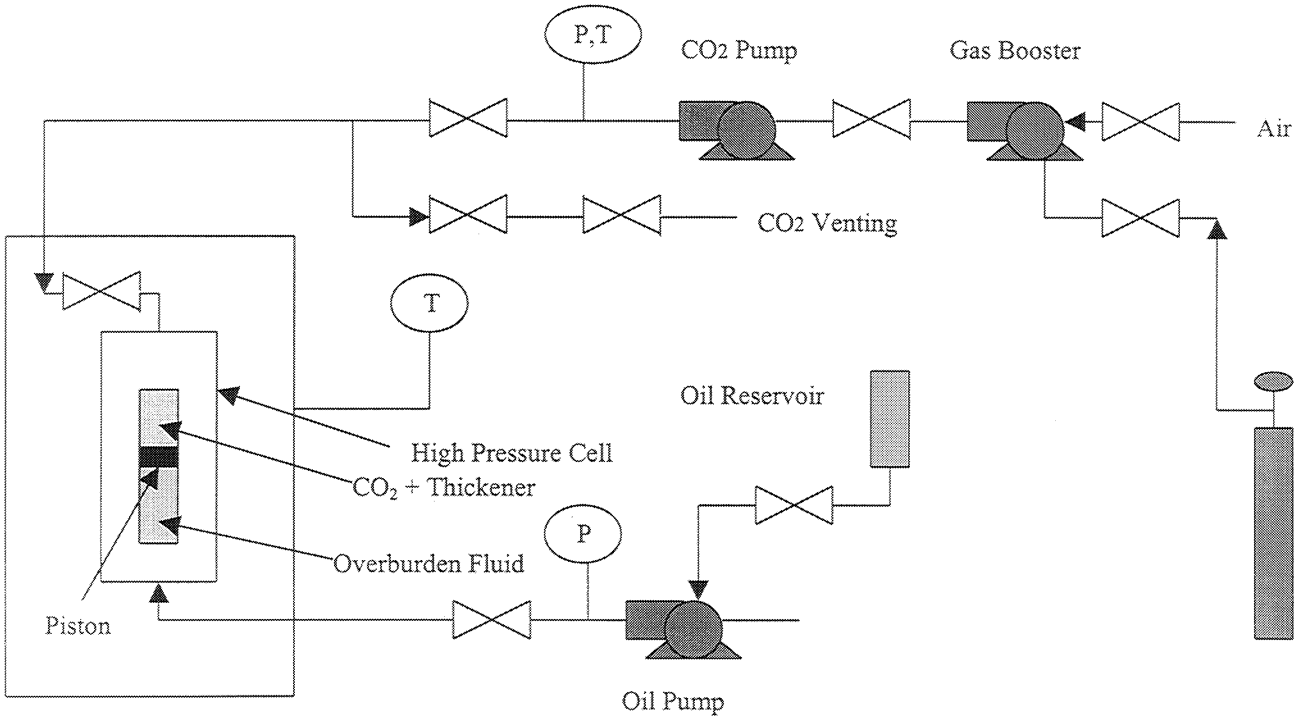


Fig.2. Experimental layout for solubility/phase behavior measurements in a high pressure, variable volume, windowed cell (D.B. Robinson Cell)

## 4.3. Solution Relative Viscosity Measurements

### 4.3.1. Experimental set-up and measurement mechanism

The viscosity of single-phase thickener-$CO_2$ solution was determined by falling cylinder viscometry. The viscosity tests were conducted in the same apparatus used for the phase behavior experiments, shown is Fig.9. This technique was selected because of its simplicity in monitoring large viscosity increases in fluids as indicated by reductions in the terminal velocity of a falling object. Visual observations enabled the verification that the reduced terminal velocity, $u_t$, was attributed to solution viscosity increase, and not insoluble sample particles inhibiting the fall.

The governing equation for the viscometer, shown as equation (1), relates the fluid viscosity $\mu$, to the product of the calibration constant, K and the density difference between the cylinder and the fluid, ($\rho_c$ - $\rho_l$ ) divided by the terminal velocity of the cylinder, $u_t$ .

$$\mu = \frac{K(\rho_S - \rho_l)}{u_t} \qquad (1)$$

The assumptions for the derivation of the above equation are:

(1) Changes in the solution density relative to that of neat carbon dioxide were assumed to be small relative to the density difference between aluminum falling cylinder and carbon dioxide;

(2) The cylinder has a uniform diameter and falls coaxially through the quartz tube;

(3) The cylinder reaches its terminal velocity instantaneously and falls in a steady state. No turbulence is present;

(4) The fluid is Newtonian in nature.

By combining the solution to the Navier-Stokes equation for laminar, annular fluid flow in a cylindrical, falling cylinder system with a force balance on the falling cylinder and a mass balance relating the displacement of fluid by the cylinder to flow through the annulus, the calibration constant can be calculated. By measuring the terminal velocity of cylinder falling through pure carbon dioxide at constant temperature and pressure, the constant can be determined experimentally. The calibration constant for our falling cylinder viscometer (cylinder diameter = 1.2438 inch) was determined experimentally to be $3.3 \pm 0.3 * 10^{-4}$ $cm^3/s^2$. While the calculated value was $2.2 \pm 0.24 * 10^{-4}$ $cm^3/s^2$. The difference can be attributed to the uneven thickness of the annular area, which in turn is related to the non-coaxial fall of the cylinder through the glass tube and variations in the diameter of the aluminum cylinder.

In a typical viscosity measurement, an aluminum cylinder was put into the cylindrical sample volume before the sample and the mixing balls were added. After equilibration of the system and the single phase was achieved, the cell was rapidly inverted and the

terminal velocity of the cylinder was measured (see schematic diagram in Fig. 12.). The solution relative viscosity, defined as the ratio of solution viscosity to neat carbon dioxide

$$\frac{\eta_{solution}}{\eta_{CO_2}} = \frac{u_{t,CO_2}}{u_{t,solution}} = \frac{t_{solution}}{t_{CO_2}} \qquad (2)$$

viscosity, was equated to the reciprocal of the terminal velocity ratio, which in turn was equated to the ratio of falling time in sample solution to falling time in pure carbon dioxide when the distance is fixed. The relationship is indicated in equation (2).

The fall time was recorded for the cylinder to fall through a fixed distance. The experiment was repeated at least six times at each concentration and the average relative viscosity results were reported.

### 4.3.2. Solution relative viscosity results

The relative solution viscosity results for tris(2-perfluorobutyl ethyl)tin fluoride were also presented in Fig. 10. The experimental results proved that tris(2-perfluorobutyl ethyl)tin fluoride was an effective thickener for liquid carbon dioxide. The solution viscosity was increased by 3.3 times at a thickener concentration as low as 4wt%.

The increase of solution relative viscosity tends to level off, however, at higher concentrations instead of going up exponentially until gel formation as observed in trialkyltin fluoride in alkane solvents. The reason is that the fluorine atoms at chain ends

may compete with the fluorine adjacent to the tin to associate with the tin atom, thus disrupting the formation of long pseudo-polymer chain.

## 4.4.Conclusions

Tris(2-perfluorobutyl ethyl)tin fluoride was soluble in liquid carbon dioxide at room temperature and a pressure below 18 MPa. However, tris(3-perfluoromethyl propyl)tin fluoride was not soluble in liquid $CO_2$ even at a pressure of 48 MPa, the highest available system pressure. The cloud point pressure v.s. composition curve (P-x diagram) is shown in Fig. 10. An examination of the phase behavior of tris(2-perfluorobutyl ethyl)tin fluoride in liquid carbon dioxide has shown that the incorporation of fluoroalkyl end groups has greatly enhanced the solubility of the trialkyltin fluoride in carbon dioxide. At a pressure as low as 18 MPa, tris(2-perfluorobutyl ethyl)tin fluoride was completely miscible with carbon dioxide up to a concentration of 5wt%. The slight decrease in cloud point pressure with an increase of concentration may be due to the closeness of the experimental region to bubble point locus region. (see insert, Fig. 3.)

The apparent distinct solubility of tris(2-perfluorobutyl ethyl)tin fluoride and tris(3-perfluoromethyl propyl)tin fluoride lies in their molecular structures. With 9 fluorine atoms at every chain end (a total of 27 in one molecule), the semi-fluorinated trialkyltin fluoride became soluble in carbon dioxide. While in tris(3-perfluoromethyl propyl)tin fluoride, only the chain end carbon was fluorinated (3 fluorine atoms at every chain and a

total of 9 in one molecule). We believe that in this case the $CO_2$-philic fluoroalkyl functionality is simply not adequate to impart observable solubility in carbon dioxide.

In summary, by introducing fluoroalkyl functionality into the tralkyltin fluoride molecular structure, the final tris(2-perfluorobutyl ethyl)tin fluoride compound was highly soluble in liquid carbon dioxide at moderate pressures. It is believed that some degree of intermolecular association through Sn-F bridging did occur so that the solution viscosity was raised by 3.3 times at a concentration of 4wt% with this low molecular weight compound. We also speculate that the fluorine atoms at the chain ends may disrupt the formation of associated polymeric chain structure by competing to associate with the tin atoms, leading to the inability of gel formation at low concentrations. From our experiment, we also postulate that an optimal length and position of fluoroalkyl substitute should exist to ensure that the compound has a high solubility in carbon dioxide, yet the fluorine atoms in the side chain have very little disrupting effect for intermolecular association.

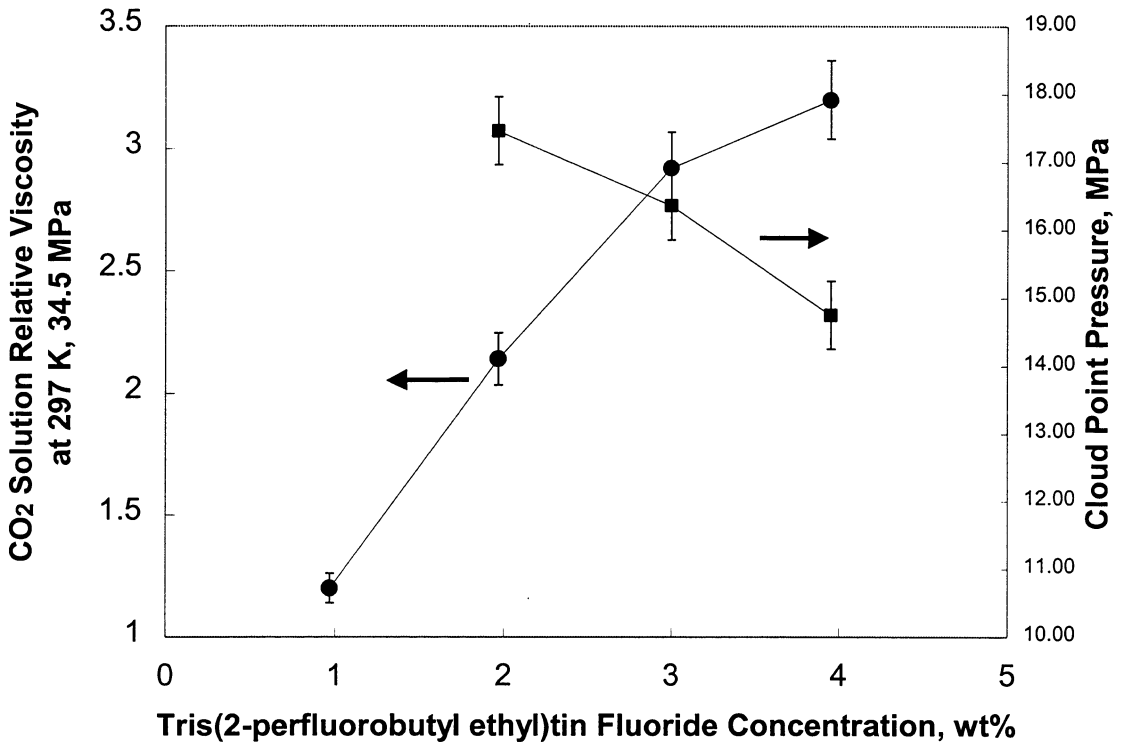


Fig. 3. Solubility and solution relative viscosity of tris(2-perfluorobutyl ethyl)tin fluoride in liquid carbon dioixde

# 5. EVALUATION OF FLUORINATED TELECHELIC DISULFATE AS DIRECT CARBON DIOXIDE THICKENERS

## 5.1.Synthesis and Characterization

### 5.1.1. Materials

(1) Fluorinated prepolymers and monomer

The precursors for the fluorinated polyurethane backbones were fluorinated diol and diisocyanate macromonomers. They were purchased from Ausimont under the trade name of Fluorolink D and B. Fluorolink D is a difunctional, hydroxyl-terminated fluorinated polyether with an average molecular weight of 2000 g/mol. Fluorolink B is a difunctional, isocyanate terminated fluorinated polyether with an average molecular weight of 3000 g/mol. The detailed molecular structure for fluorinated prepolymers are as follows:

Fluorolink D: $HOCH_2CF_2(R_1)_p(R_2)_qCF_2CH_2OH$

Fluorolink B: $OCN\text{-}Ar\text{-}OCCF_2O(R_1)_p(R_2)_qCF_2CONH\text{-}Ar\text{-}NCO$

The aromatic group in Fluorolink B structure is a 2-methyl phenyl group. Here $R_1$ is $CF_2CF_2O$, $R_2$ is $CF_2O$, p/q = 0.8. Both prepolymers have difunctional contents greater than 95% and unspecified polydispersities.

The monomer used for the synthesis of negative control polymer was heptadecafluorodecyl acrylate. The monomer was obtained from Aldrich and inhibited with 100ppm monomethyl ether hydroquinone. The inhibitor was removed by washing

with 5% aqueous NaOH solution. The monomer was subsequently dried over $MgSO_4$ and stored in a fridge before polymerization.

(2) Other reagents and solvents

1,6-Bis(diisocyanato hexane) (HDI), dibutyltin dilaurate, chlorosulfonic acid, and sodium methoxide (25 wt% solution in methanol) were all purchased from Aldrich and used as received. 2, 2′-azobisisobutyronitrile (AIBN) was recrystallized from methanol twice before use. Argon was ordered from Praxair and passed through a $CaCl_2$ drying tube before use. All other solvents were obtained from Aldrich and used as received.

### 5.1.2. Reactions

The reaction route to obtain final telechelic disulfates with different molecular weights is presented in Fig.13. The stoichiometric ratios used to synthesize diols with different molecular weights were tabulated in Table 1. First, diols were chain extended with diisocyanates, either fluorolink B or HDI. Followed by molecular weight determination, the extended diols were then transformed to disulfuric acids and subsequently neutralized to give polyurethane based telechelic sodium disulfates.

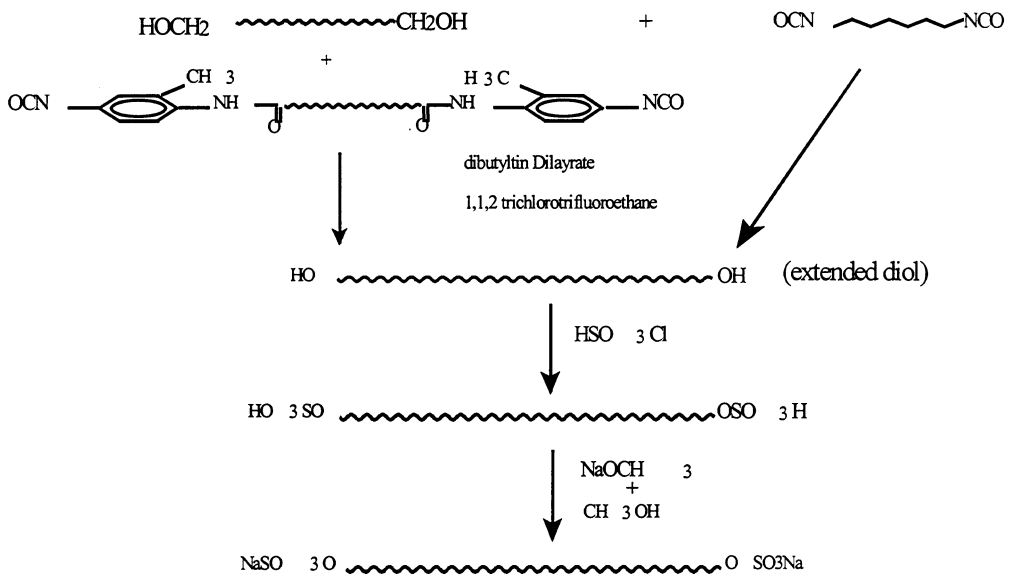


Fig. 1. Synthetic route of polyurethane telechelic disulfates

| $N_{OH}$, mmol | $N_{NCO}$, mmol | $N_{NCO}/N_{OH}$ | $MW^{cal}$ | $MW^{exp}$ |
|---|---|---|---|---|
| 5 | 3.735 | 0.747 | 15,200 | 13,800 |
| 5 | 3.895 | 0.779 | 17,700 | 15,400 |
| 5 | 3.980 | 0.796 | 19,300 | 18,700 |
| 5 | 4.865 | 0.873 | 32,500 | 29,900 |

Table 1. Stoichiometric ratios of HDI extended diols with different molecular weights $MW^{cal}=M_0X_n + M_{eg}$, where $M_0=2196$, $M_{eg}=0$, $X_n=(1+r)/(1-r)$ by assuming conversion $p=1$.

### 5.1.3. Procedures

#### 5.1.3.1. Extended diol formation

Take the synthesis of HDI extended diol ($MW^{cal}$ = 19,300) as an example, the syntheses of other diols with different molecular weights are similar except that different Fluorolink D and HDI ratios were used.

Typically, in a 100ml three-neck flask equipped with a stirring bar, charge 10g Fluorolink D diol (5 mmol). 30ml 1,1,2-trichlorotrifluoroethane (hereafter called Freon 113 or Freon) was then added to the flask. Star stirring until the diol was dissolved. Three drops of dibutyltin dilaurate were added through a pipette to the solution. Start heating until reflux (~48 $^0$C) in an argon blanket. Through the septum, charge 0.766ml HDI dropwise to the reaction mixture via a 1 ml syringe with minimum calibration as 0.01ml. After HDI addition, the reaction mixture were allowed to reflux overnight before the heating and stirring were stopped. The reaction mixture became very viscous after overnight reaction. The viscous reaction mixture was then precipitated into 100ml chloroform three times and dried in the vacuum oven for two days.

Characterization with NMR spectra showed down field chemical shifts from tetramethylsilane at 3.88 ppm for methylene proton $CF_2C\mathbf{H_2}OH$, 4.62 ppm for hydroxy proton $CF_2CH_2O\mathbf{H}$. NMR spectra for HDI extended diol ($MW^{cal}$ = 19,300) showed again

these two chemical shifts at 4.50 ppm and 3.32 ppm, respectively; and also chemical shifts from HDI backbone at 1.48 and 1.20 for methylene protons, NHCOC**H**$_2$C**H**$_2$C**H**$_2$, and a broad peak centered at 5.62 ppm for urethane proton N**H**COCH$_2$. IR characterization also confirmed the extended structure. Typical absorbance due to isocyanate carbonyl at 2280 cm$^{-1}$ disappeared. The IR spectra showed urethane carbonyl absorbance at 1724.7 cm$^{-1}$ and 1535.6 cm$^{-1}$; O-H stretching at 3470.5 cm$^{-1}$, N-H stretching at 3346 cm$^{-1}$, and C-H stretching absorbance at 2940 cm$^{-1}$, respectively.

### 5.1.3.2. Extended diol molecular weight determination

The molecular weight of the extended diols was determined by end group titration method. End group analysis is applicable to our diol system because the existence of hydroxyl end groups in the polymer molecules and low designed polymer molecular weight ($M_n$ < 50,000). Typically, in a titration procedure for our extended diols, around 1g of a diol sample was dissolved in a minimum amount of freon, usually about 20ml. The dissolved diol was allowed to react with 10 times excess amount of acetic anhydride to form an acetic ester. The residual acetic anhydride was later on titrated with 0.1007 M standard alcoholic KOH solution to reach a phenolphthalein endpoint in a freon-acetone solution. The volume of KOH solution was recorded and the experiment was repeated three times for a given diol polymer sample. The KOH solution volume can be related to diol molecular weight in equation (3):

$$\overline{M}_{n,diol}(g/mol) = \frac{w_{diol}(g) \times 2(difunctional) \times 10}{V_{KOH}(ml) \times 0.001(L/ml) \times 0.1007(mol/L)} \qquad (3)$$

Here the number 10 in the numerator means that the acetic anhydride is 10 times more than needed for esterification. The amounts of acetic anhydride and KOH solution used for each diol sample were presented in Table 2.

| $M_n^{cal}$, g/mol | $w_{diol}$, g | $N_{OH}$, mmol | $V_{(CH3CO)2O}$, ml | $V_{KOH}$, ml | $M_n^{exp}$, g/mol |
|---|---|---|---|---|---|
| 15,200 | 1.01 | 0.01316 | 0.137 | 14.55 | 13,800 |
| 17,700 | 1.01 | 0.01130 | 0.117 | 13.00 | 15,400 |
| 19,300 | 1.01 | 0.01036 | 0.108 | 10.71 | 18,700 |
| 32,500 | 1.04 | 0.00615 | 0.064 | 6.90 | 29,900 |

Table 2. Reagent amounts for diol MW determination by end-group titration

### 5.1.3.3. Acidification and neutralization

After the molecular weight of the diol samples was determined by experiments, the diols were then subjected to acidifcation by chlorosulfuic acid and further neutralized by sodium methoxide, 25wt% solution in methanol. The reagent amounts were shown in Table 3. for diols with different molecular weights.

For example, for diol with an experimental MW of 18,700, typically, 3.46g (0.185 mmol) diol sample was first dissolved in 30ml Freon. 0.100ml chlorosulfonic acid (0.74mmol) was added dropwise to the diol solution. The reaction mixture was stirred at room temperature for 6 hours. By the end of the reaction, a precipitated viscous polymer phase was obtained. The solvent was removed under vacuum and the polymer left was washed with acetone to remove residual unreacted acid. The polymer was re-dissolved in freon-methanol mixture (1:1 v/v), and neutralized with $NaOCH_3$, 25wt% solution in methanol to a phenolphthalein indicated end-point.

| $M_n^{exp}$, g/mol | $w_{diol}$, g | $V_{HClSO3}$, ml | $V_{NaOCH3}$, ml |
|---|---|---|---|
| 13,800 | 3.30 | 0.130 | 0.109 |
| 15,400 | 3.01 | 0.106 | 0.089 |
| 18,700 | 3.46 | 0.100 | 0.085 |
| 29,900 | 3.03 | 0.055 | 0.046 |

Table 3. Reagent amounts for acidification and neutralization of extended diols

NMR spectra for telechelic disulfates showed the disappearance of alcohol proton at 4.62ppm and the downfield shift for other polymer backbone protons. IR spectra shoed the disappearance of O-H stretching absorbance at 3470 $cm^{-1}$. (see Appendix A.)

### 5.1.4. Synthesis of poly(heptadecafluorodecyl acrylate)

Poly(heptadecafluorodecyl acrylate) was synthesized in α,α,α-trifluorotoluene. This polymer served as a control for solubility and viscosity study of polyurethane telechelic disulfates.

In a typical experiment, 10g heptadecafluorodecyl acrylate monomer and 5mg initiator AIBN were measured and transferred into a 50ml ampule. 10ml of trifluorotoluene was then added. The reaction mixture was subsequently purged with argon for 5min and sealed with flame. The reaction was carried out in an oil bath at 60-65$^0$C for 24 hours. After reaction, the polymer solution was precipitated into 300ml methanol three times and the obtained polymer was then dried in a vacuum oven overnight. The product polymer is a white powder, yield 84%. The MW of the polymer was not determined experimentally.

## 5.2. Phase Behavior of Polyurethane Telechelic Disulfates in Carbon Dioxide

### 5.2.1. Experimental set-up

The experimental set-up of the phase behavior study with polyurethane telechelic disulfates is the same as shown in Chapter 4.2.1. The disulfate samples were left in liquid

CO2 at a pressure of 6,800 psi overnight and mixed for at least 30min before cloud points pressures were measured.

### 5.2.2. Results and Discussions

Fluorolink D was initially transformed to disulfate following the same procedure. But the obtained disulfate product was not soluble in carbon dioxide at room temperature and the maximum achievable pressure in our apparatus. The fluorolink D diol was further extended with fluorolink B, a fluorinated diisocyanate discribed in the previous chapter. The extended disulfates (trimer and pentamer) synthesized in this way still exhibited marginal solubility in carbon dioxide up to 7000 psi. This led to our consideration that the $CO_2$-phobic aromatic groups at each diisocyanate block may prohibit the sample from dissolving. To make the extended disulfate more soluble at moderate pressures and to have a better control over their molecular weight, a short chain alkyl diisocyanate, HDI was used instead as a chain extender.

The phase behaviors of polyurethane telechelic disulfates were presented in Fig. 3, with the cloud points pressures recorded for the four $CO_2$ soluble HDI extended disulfates. A single phase liquid occurred at conditions above the dew point (cloud point) locus, while liquid-liquid phase equilibrium existed at conditions below the dew point pressure. The disulfate ionomer with MW of 13,800 was the lowest MW sample in our series that was soluble in liquid carbon dioxide below 50 MPa. As the molecular weight increased from 13,800 to 15,400 and then to 18,700 g/mol, the cloud point pressure decreased

significantly. The increased miscibility with increasing molecular weight can be attributed to the enhanced carbon dioxide-philicity of the ionomer. As the molecular weight increases from 13,800 to 18,700, the increase of $CO_2$-philic fluorinated polyurethane content dominates, rendering the whole molecule greater solubility in carbon dioxide despite the molecular weight increase. Over a certain molecular weight value, however, the unfavorable entropy of mixing associated with high molecular weight polymer in $CO_2$ system dominates, therefore the disulfate became less soluble in carbon dioxide and the pressure needed for solubilization at a certain concentration increases. There exits an optimal molecular weight where the two effects are balanced in such a way that the greatest solubility can be achieved. This observation has been previously substantiated by other researchers working with $CO_2$ soluble amphiphilic polymers.

As a comparison, polyfluoroacrylate polymerized in trifluorotoluene was very soluble in liquid $CO_2$ as indicated by the much lower cloud point pressure (below 10 MPa) up to a concentration of 5wt%. This high solubility is in agreement with the fluoropolymer solubility results of DeSimone and Mawson, et al.

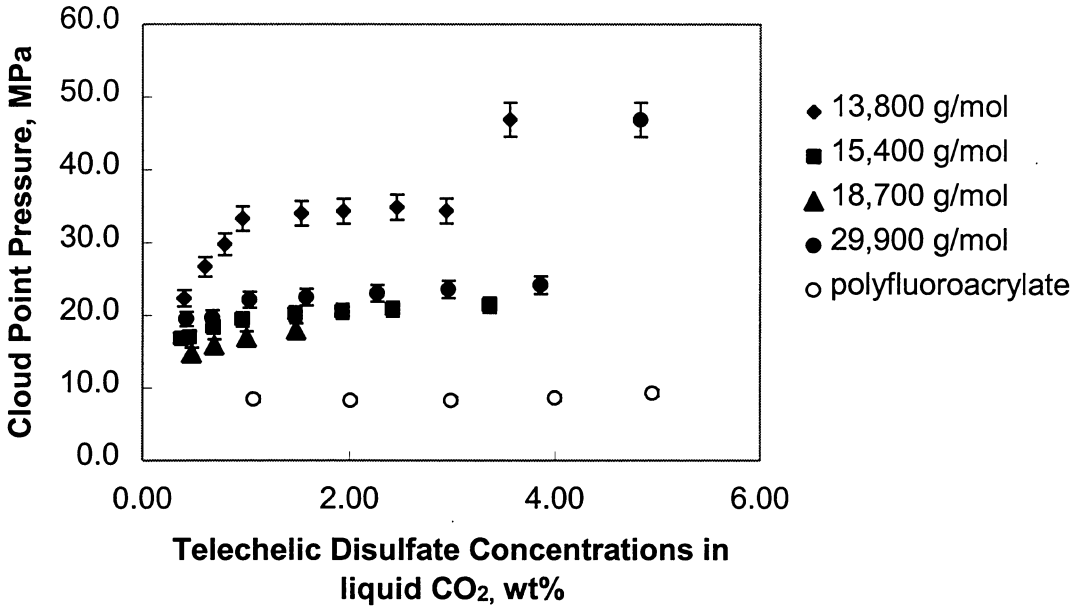


Fig.2. Phase behavior of polyurethane telechelic disulfates in liquid carbon dioxide, T=297 K.

## 5.3. Solution Relative Viscosity Measurements

The experimental set-up and mechanism for solution relative viscosity measurements were shown previously in Chapter 4.3.1. The fluorinated polyurethane telechelic disulfates were allowed to stay in liquid carbon dioxide at a pressure of 6,800 psi overnight and mixed by rocking the high pressure cell for at least 30min before solution relative viscosity was measured.

The solution relative viscosity results were shown in Fig. 4. The polymer has a molecular weight of 29,900 as determined by titration experiments. The relative viscosity of single-phase mixtures of $CO_2$ and fluorinated polyurethane disulfate was measured at 298 K and 34.5 MPa in the concentration range between 0wt% (neat CO2) to 4wt%. Beyond 4wt% the disulfate was not soluble in $CO_2$ below 7000 psi. as shown previously in Fig.14. Below 1wt%, the ionomer-CO2 solution relative viscosity was quite close to that of neat carbon dioxide at the same conditions. However, there is a significant viscosity jump when the concentration increased from 2wt% to 4wt%, leading to relative viscosity increment at 4wt% by a factor of 2.7.

The viscosity results indicated that the $CO_2$-soluble fluorinated polyurethane telechelic disulfate was capable of significantly increasing the viscosity of $CO_2$ at relatively low

concentrations. Although the relative viscosity exhibited a sharp increase at concentrations higher than 2 wt%, further viscosity increases at higher concentrations

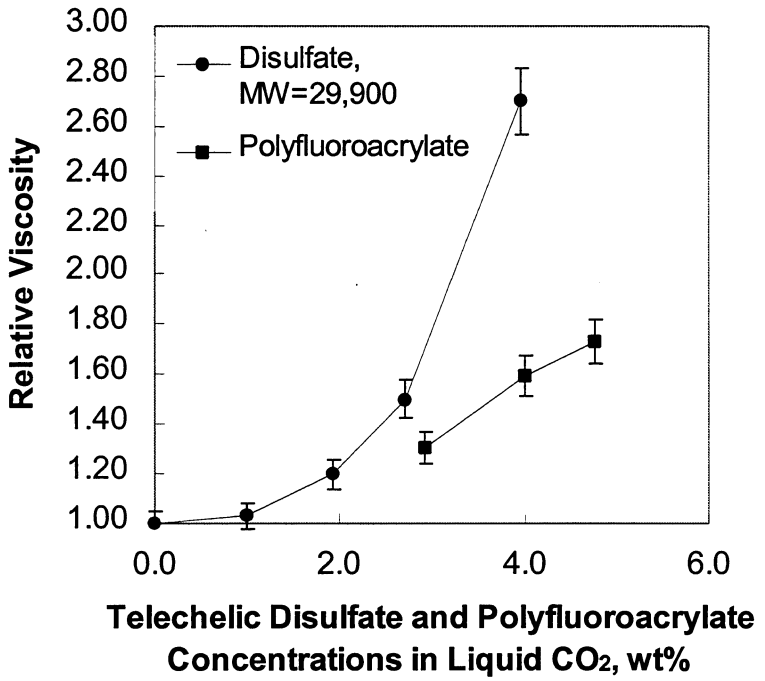


Fig. 4. Solution relative viscosity results for fluorinated polyurethane telechelic disulfates; the relative viscosity of poly(heptadecafluorodecyl acrylate) in carbon dioxide solution was also presented here for comparison.

were not attained because the solubility limit of the telechelic ionomer in carbon dioxide was below 5wt% under our experimental conditions.

For comparison, the relative viscosity of poly(heptadecafluorodecyl acrylate)-$CO_2$ solution was also recorded. Although the polymer molecular weight is higher than that of telechelic disulfates, the degree of solution viscosity increase was less than that achieved with the disulfate at an equivalent concentration. The comparison results showed that although high molecular weight polymer can increase liquid carbon dioxide viscosity by chain entanglement, they are not effective carbon dioxide thickeners at low concentrations. Fluorinated polyurethane disulfates, however, are more effective thickeners because they have $CO_2$-phobic disulfate groups that tend to associate in a carbon dioxide solution.

## 5.4.Conclusions

By introducing $CO_2$-philic fluoroether functionality into the structure of polyurethane telechelic disulfate, the compound exhibited substantial solubility (up to 4wt%) in liquid carbon dioxide at pressure lower than 7000 psi, despite the existence of ionic ($CO_2$-phobic) end groups. There exists an optimal molecular weight where the fluorinated disulfate exhibited the highest solubility in carbon dioxide. Below this molecular weight, the CO2-philic fluoroether content dominates, and the polymer were more soluble in CO2

as the molecular weight increases; Above this molecular weight, the higher the polymer molecular weight, the lower the solubility because of the unfavorable entropy of mixing.

The solution viscosity of disulfate (MW = 29,900) showed a 2.7 times increase at a concentration of 4wt%. By comparing the viscosity increases resulted from both the disulfate and the high molecular weight poly(heptadecafluorodecyl acrylate), we concluded that relatively low molecular weight ionomers are more effective than high molecular weight random coil polymers in solution viscosity increase. We speculate that the $CO_2$-phobic disulfate end groups may promote intermolecular association in a carbon dioxide environment to give a significant solution relative viscosity at low concentrations, while the chain entanglement for high molecular weight $CO_2$-soluble polymers will not easily occur unless the concentration are very high.

# 6. EVALUATION OF FLUOROALKYL ASPARTATE BISUREAS AND UREAS FOR CARBON DIOXIDE THICKENING AND MICROCELLULAR FOAM GENERATION

## 6.1. Synthesis and Characterization

### 6.1.1. Materials

N-t-BOC protected aspartic acid (N-t-BOC-L-Asp) and N-CBZ protected aspartic acid (N-CBZ-L-Asp) were obtained from SIGMA and stored below 0 $^0$C in the fridge before use. 1H,1H,2H,2H-Perfluorodecanol (97%) was purchased from Lancaster Synthesis. Hexafluoropropylene oxide homopolymer alcohol (MW=1200 g/mol, fluoroether monofunctional alcohol, DuPont product, brand name Krytox, 95%) was purchased from Miller-Stephenson; 1-[3-(Dimethylamino)propyl]-3-ethylcarbondiimide hydrochloride (EDCI, 98+%) and 4-(Dimethylamino)pyridine (DMAP, 99+%) were both ordered from Aldrich; Palladium hydroxide, 20 wt% Pd (dry basis) on carbon (Pearlman's catalyst) was obtained from Aldrich; Diisocyanates and isocyanates used in our synthesis were purchased from Aldrich. All other chemicals and solvents were obtained from Aldrich and used as received.

### 6.1.2. Reactions

The reaction routes for the synthesis of fluorinated aspartate bisureas and ureas were generalized in Fig. 1. To synthesize a bisurea, a diisocyanate was reacted with the deprotected aspartate; To synthesize a urea, an isocyanate was the reactant instead.

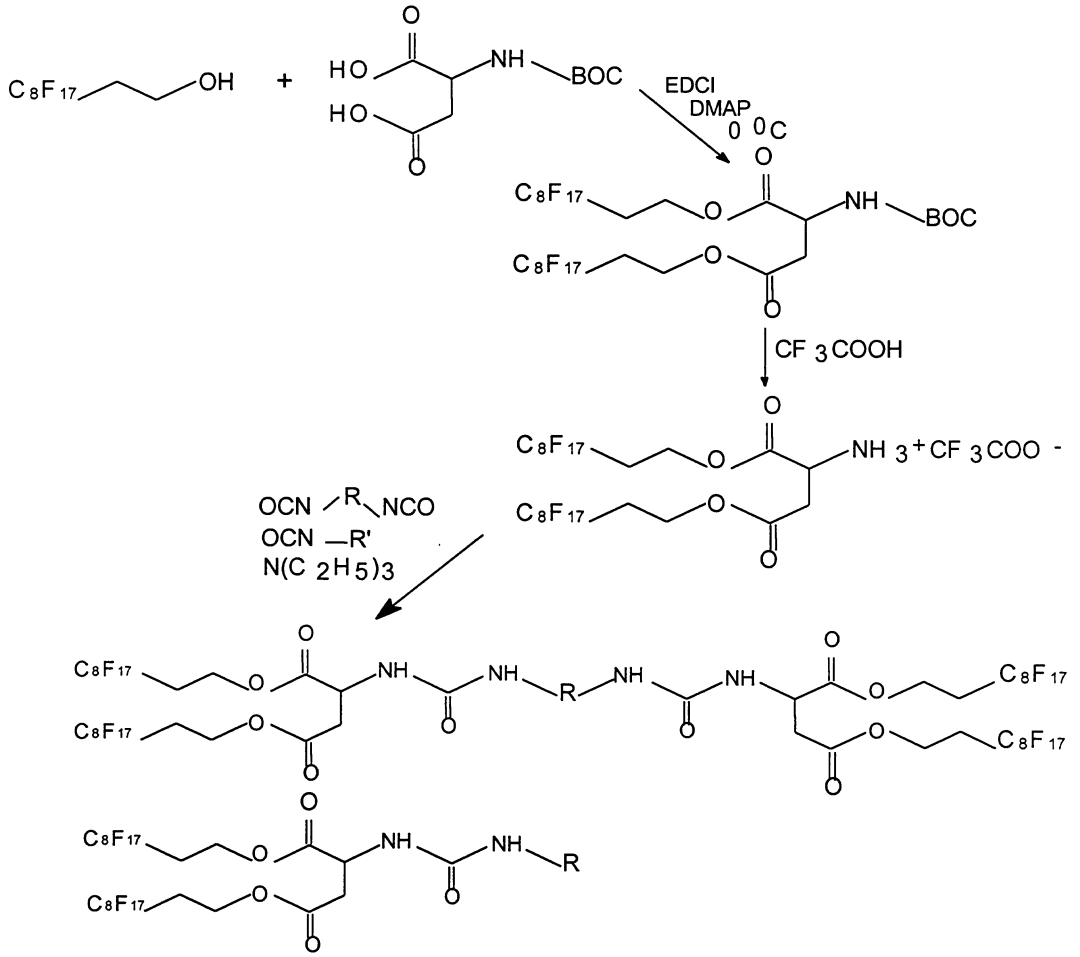


Fig.1. Synthetic routes for fluorinated aspartate bisureas and ureas

In our synthesis, both short chain (FW = 464g/mol) fluoroalkyl alcohol and long chain (MW = 1,200) fluoroether alcohol were used to introduce the $CO_2$-philic functionalities into the bisureas and ureas structures. Different diisocyanates and isocyanates were also used to give various $CO_2$-phobic strucutres. The synthesized bisureas were listed in Table 1. The synthesized ureas were listed in Table 2.

| $CO_2$-phile | R group | Freon 113 | | PFDMCH | |
|---|---|---|---|---|---|
| | | Soluble? | Gel? | Soluble? | Gel? |
| $CF_3(CH_2)_7(CH_2)_2$ | $(CH_2)_6$ | no | no | no | yes |
| $CF_3(CH_2)_7(CH_2)_2$ | $(CH_2)_{12}$ | no | no | no | yes |
| $CF_3(CH_2)_7(CH_2)_2$ | 1,4-phenyl | no | no | no | yes |
| $CF_3(CH_2)_7(CH_2)_2$ | 1,4-xylyl | no | no | no | yes |
| $CF_3(CH_2)_7(CH_2)_2$ | Fluoroether[b] | no | no | no | loose fibers |
| fluoroether[a] | $(CH_2)_6$ | yes | no | yes | no |

Table 1. Fluorinated aspartate biureas synthesized; The solubility and gelling behavior at 1wt% concentrations of theses biureas in freon 113 and PFDMCH (perfluoro-1,3 dimethyl cyclohexane) were also listed as a screening test before evaluation in carbon dioxide.

a. Hexafluoropropylene oxide homopolymer alcohol, MW=1200

b. Fluorolink B, as described in Chapter 5.1.1., MW=3000

| $CO_2$-phile | R group | Freon 113 | | PFDMCH | |
|---|---|---|---|---|---|
| | | Soluble? | Gel? | Soluble? | Gel? |
| $CF_3(CH_2)_7(CH_2)_2$ | *p*-fluoro-phenyl | no | yes | no | yes |
| $CF_3(CH_2)_7(CH_2)_2$ | *p*-$CF_3$-phenyl | no | no | no | no |
| $CF_3(CH_2)_7(CH_2)_2$ | 3,5-$(CF_3)_2$-phenyl | no | yes | no | yes |
| $CF_3(CH_2)_7(CH_2)_2$ | $CH_3(CH_2)_5$ | yes | yes | no | yes |
| $CF_3(CH_2)_7(CH_2)_2$ | phenyl | no | yes | no | yes |
| $CF_3(CH_2)_7(CH_2)_2$ | Ethyl methacrylate | no | no | no | yes |
| Fluoroether[a] | 3,5-$(CF_3)_2$-phenyl | yes | no | yes | no |
| Fluoroether[a] | $CH_3(CH_2)_5$ | yes | no | yes | no |

Table 2. Fluorinated aspartate ureas synthesized; The solubility and gelling behavior at 1wt% concentrations of theses biureas in freon 113 and PFDMCH (perfluoro-1,3 dimethyl cyclohexane) were also listed as a screening test before evaluation in carbon dioxide.

a. Hexafluoropropylene oxide homopolymer alcohol, MW=1200

### 6.1.3. Procedures

(1) Synthesis of Deprotected Fluoroalkyl Aspartate Amine

Typically, in a 250ml 3-neck flask equipped with a stirring bar, charge 100ml dichloromethane. 7.88g 1H,1H,2H,2H-perfluorodecanol (0.017mol) was added and the flask was cooled in an ice bath. 2g N-Boc-Asp (0.0086mol) and 3.28g (0.017mol) EDCI were subsequently charged to the reaction mixture. Start stirring until most of the reactants were dissolved. 1.05g DMAP (0.0086mol) was then introduced. The reaction mixture was kept in the ice bath for 30 min, then the ice bath was removed and reaction was kept at room temperature overnight.

The reaction mixture was then diluted with 100ml chloroform and transferred to a separation funnel. The organic layer was washed with 50ml 1%HCl twice, and 50ml brine once and dried over sodium sulfate. Solvents were later removed under vacuum to yield a pale yellow solid. The solid was then dissolved in a minimal amount of dichloromethane (Freon was added if necessary). The obtained solution was transferred to a silica column and washed with chloroform. Solvent was subsequently removed under vacuum and a white solid aspartate product was obtained with 80% yield.

The obtained aspartate diester was subject to deprotection with trifluoroacetic acid. Typically, 5g aspartate was deprotected with 10ml trifluoroaceticacid in 20ml dichloromethane for 4 hours. The solvent was removed under reduced pressure. Chloroform was added and removed under vacuum until a white solid formed. The solid was then recrystallized from 200ml ethanol and cooled to room temperature and stored in a fridge for 3 hours. The solid was collected and dried under reduced pressure. The deprotected aspartate amine was a needle-shaped white solid with 78% yield.

$^1H$ NMR spectra taken from a Bruker 300 MHz NMR showed 4.87ppm ($O{=}C(C\mathbf{H})CH_2NH$ in aspartate residue), 4.58ppm ($O{=}C(C\mathbf{H_2})CH$ in aspartate residue), 4.40ppm ($C_8F_{17}CH_2(C\mathbf{H_2})O$ in fluorodecanol residue), and 2.48ppm ($C_8F_{17}(C\mathbf{H_2})CH_2$ in fluorodecanol residue).

(2) Synthesis of Deprotected Fluoroether Aspartate Amine

Similar to the synthesis of fluoroalkyl aspartate, fluoroether aspartate was synthesized in 100ml cooled ethyl acetate-1,1,2-trichlorotrifluoroethane (called in the following Freon 113) mixture (1:1 v/v) with fluoroether alcohol and N-CBZ-Asp as the reactants. After reaction, most solvents were removed and the concentrated oil was washed with 50ml ethyl acetate twice, 50ml ethanol once, and 100ml 1% HCl twice. The residue was then diluted with 50ml freon and dried over sodium sulfate. Vacuum evaporate most freon 113 until the residue reached a volume of 20-30ml. The yellow-colored solution was then purified over a silica column and washed down with 1:1 ethyl acetate-freon mixture. Solvents were later evaporated and yield a colorless oil.

The fluoroether aspartate diester was then deprotected by hydrogenation with Pd(OH)2/C as the catalyst. Typically, 5.0g fluoroether aspartate diester was dissolved in 20ml perfluoro1,3-dimethyl cyclohexane, 0.25g palladium hydroxide on carbon catalyst was added. Start stirring vigorously. $N_2$ was passed through the reaction flask to displace air before hydrogen was introduced. The diester was deprotected with hydrogen for 12 hours, then the catalyst was removed first by filtration (Whatman #1 filter), then the

residual fine catalyst particles were removed by Millipore membrane filter (0.45μm). The solvent was removed under vacuum and residue washed with ether. Yellowish oil sample was then dried under vacuum.

$^1$H NMR spectra showed peaks at 7.22ppm ($C_6\mathbf{H_5}CH_2$ in CBZ-Asp residue), 5.99ppm ($CF_2(C\mathbf{H_2})O$ from fluoroether alcohol residue), 5.00ppm ($O{=}C(C\mathbf{H_2})CH$ in aspartate residue), 4.34ppm ($O{=}C(C\mathbf{H})CH_2NH$ in aspartate residue), 4.69ppm ($CH(N\mathbf{H})C{=}O$ from aspartate residue), and 2.93ppm ($O(C\mathbf{H2})C_6H_5$ from CBZ-Asp residue).

(3) Synthesis of Bisureas and Ureas

The deprotected fluoroalkyl or fluoroether aspartate amines were than reacted with stoichiometric amounts of commercially available diisocyanates and isocyanates to yield biureas and ureas of different structures.

Typically, the reactions between deprotected fluoroalkyl aspartate amine and diisocyanates/isocyanates were carried out in 50ml dichloromethane with triethylamine as the catalyst. The product fluoroalkyl bisureas/ureas are white solids and collected by filtration and washed with 1% HCl and hexanes and then dried under vacuum. The fluoroether bisureas/ureas were obtained by reacting the deprotected fluoroether amine with different diisocyanates/isocyanates in 50ml freon 113, with triethylamine as the catalyst. After reactions, solvent was removed by reduced pressure and the oily product washed with 1% HCl and hexanes and dried.

The synthesized biureas/ureas were charaterized by taking IR spectra on a Mattson Polaris FT-IR. Solid samples were mixed with KBr and compressed into pellets before taking the spectra. Liquid samples were prepared in the form of thin films between NaCl windows.

The IR spectra for fluoroalkyl biureas/ureas are similar, showing N-H streching absorbance at 3350-3360 $cm^{-1}$, C-H stretching at 2940-2990 $cm^{-1}$, carbonyl absorbance around 1735-1745 $cm^{-1}$, N-H scissoring absorbances at 1630 and 1570 $cm^{-1}$ respectively.

The IR spectra for fluoroether bisureas/ureas usually show N-H streching absorbances at 3340-3350 $cm^{-1}$, C-H strecthing at 2940-2980 $cm^{-1}$, carbonyl absorbance around 1760-1770 $cm^{-1}$, and two N-H scissoring absorbances at 1650 and 1570 $cm^{-1}$.

The melting point for each solid urea/bisurea sample was measured in a TA Instrument DSC 2910 with indium as the reference and nitrogen as the purging gas. The heating rate was 10 $^{0}$C/min.

## 6.2. Phase Behaviors of Fluorinated Aspartate Bisureas and Ureas in carbon dioxide

### 6.2.1. Experimental

The experimental set-up is the same as described in Chapter 4.2.1. The solubility of every fluorinated aspartate bisurea or urea was first evaluated at room temperature and below system maximum pressure 7,000 psi. If the sample was not completely soluble at room temperature, the high pressure cell was then heated to 80 $^{0}$C or higher while keeping the pressure between 5,000 ~ 6,800 psi by expanding the sample volume until the sample

was dissolved in supercritical carbon dioxide. The resulted solution was subsequently cooled down to room temperature by keeping the pressure above 5000 psi and the behavior was recorded.

| $CO_2$-phile | R group | behavior in carbon dioxide | |
|---|---|---|---|
| | | Soluble? | behavior after cooling |
| $CF_3(CH_2)_7(CH_2)_2$ | $(CH_2)_6$ | yes, at 90 $^0$C, 6000 psi | monolith at 3.0-4.9wt%, collapsed network at 2.2wt% |
| $CF_3(CH_2)_7(CH_2)_2$ | $(CH_2)_{12}$ | yes, at 90 $^0$C, 6000 psi | collapsed network at 4.0wt% |
| $CF_3(CH_2)_7(CH_2)_2$ | 1,4-phenyl | yes, at 100 $^0$C, 6000 psi | precipitated powder at 2.0wt% |
| $CF_3(CH_2)_7(CH_2)_2$ | 1,4-xylyl | yes, at 100 $^0$C, 6000 psi | precipitated powder at 3.4wt% |
| $CF_3(CH_2)_7(CH_2)_2$ | Fluoroether[b] | yes, at 90 $^0$C, 6000 psi | loose floating fibers at 2.5wt% |
| fluoroether[a] | $(CH_2)_6$ | Yes, up to 5.0wt% at 25 $^0$C, 2000 psi | stay as a solution at 25 $^0$C, no significant viscosity increase |

Table 3. Phase behavior of fluorinated aspartate bisureas in carbon dioxide

a. Hexafluoropropylene oxide homopolymer alcohol, MW=1200

b. Fluorolink B, as described in Chapter 5.1.1., MW=3000

| $CO_2$-phile | R group | behavior in carbon dioxide | |
|---|---|---|---|
| | | Soluble? | behavior after cooling |
| $CF_3(CH_2)_7(CH_2)_2$ | *p*-fluoro-phenyl | yes, at 90 $^0$C, 6000 psi | collapsed network at 4.5wt% |
| $CF_3(CH_2)_7(CH_2)_2$ | *p*-$CF_3$-phenyl | yes, at 90 $^0$C, 6000 psi | precipitated powder at 2.5wt% |
| $CF_3(CH_2)_7(CH_2)_2$ | 3,5-$(CF_3)_2$-phenyl | yes, up to 6.0wt% at 25$^0$C, 2000 psi | collapsed network at 2.0-6.0wt% |
| $CF_3(CH_2)_7(CH_2)_2$ | $CH_3(CH_2)_5$ | yes, up to 5.0wt% at 25$^0$C, 5000psi | collapsed network at 3.7-5.0wt% |
| $CF_3(CH_2)_7(CH_2)_2$ | phenyl | yes, up to 5.1wt% at 90$^0$C, 6000 psi | monolith at 4.8-5.1wt%, collapsed network at 1.5wt% |
| $CF_3(CH_2)_7(CH_2)_2$ | Ethyl methacrylate | yes, up to 4.7wt% at 25$^0$C, 2000 psi | collapsed network at 4.7wt% |
| fluoroether[a] | 3,5-$(CF_3)_2$-phenyl | yes, up to 5wt% at 25$^0$C, 2000psi | stay as a solution at 25 $^0$C, no significant viscosity increase |
| fluoroether[a] | $CH_3(CH_2)_5$ | yes, up to 5wt% at 25$^0$C, 2000psi | stay as a solution at 25 $^0$C, no significant viscosity increase |

Table 4. Phase behavior of fluorinated aspartate ureas in carbon dioxide

a. Hexafluoropropylene oxide homopolymer alcohol, MW=1200

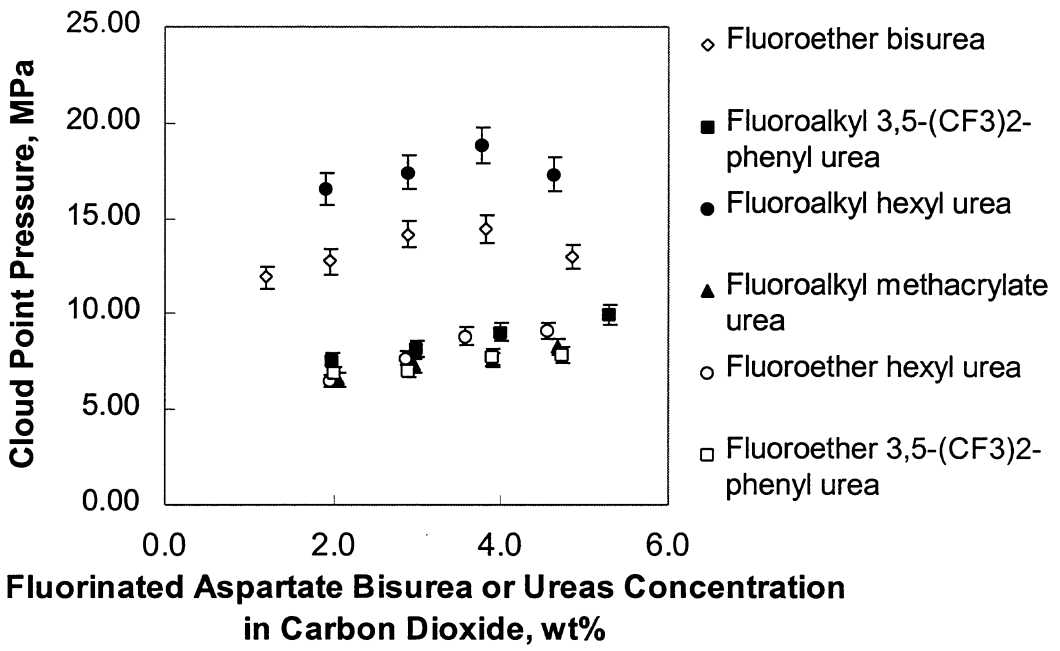


Fig. 2. Phase behavior of $CO_2$-soluble fluorinated aspartate biureas and ureas at 298 K

### 6.2.2. Results and discussions

The solubility of bisureas in carbon dioxide was listed in Table 3. The solubility of ureas in carbon dioxide was summerized in Table 4. The behaviors after cooling were also recorded in Table 3 and Table 4 for bisureas and ureas respectively. As can be seen from the tables, all of the bisureas and ureas that we evaluated can be dissolved in carbon dioxide below 48.3 MPa (7,000 psi) and at room temperature or elevated temperature. The P-x phase diagram for bisureas and ureas that were soluble in carbon dioxide at room temperature were presented in Fig. 2.

Of all these fluorinated aspartate bisureas tested, only the bisurea with fluoroether tails and HDI backbone was soluble in liquid carbon dioxide at room temperature. We believe that although both fluoroalkyl and fluoroether are $CO_2$-philic, fluoroether functionality is more $CO_2$-philic and therefore is able to impart higher solubility in carbon dioxide if the other molecular structures are the same. This was obvious when we compare the solubility of fluoroether 1,6-hexyl bisurea and fluoroalkyl 1,6-hexyl bisurea. The fluoroether version was readily soluble in carbon dioxide at room temperature with a cloud point pressure below 15 MPa, while the fluoroalkyl version was not soluble at 41.4 MPa (6,000 psi) until heated to 90 $^0$C.

Comparison among the bisureas that have the same $CO_2$-philic tail also revealed the $CO_2$-phobic trend for different backbone structures. Among them, the aryl groups such as phenyl and xylyl were more $CO_2$-phobic than the alkyl structures, as indicated by the

higher cloud point pressure after sample solubilization (data not shown). We tried to enhance the bisurea solubility by introducing fluoroether backbone into the molecular structure, but the solubility of thus synthesized bisurea was not changed much. We believe this may be due to the lower solubility of the longer chain fluoroether. The fluoroether diisocyanate were tested to require higher pressure to dissolve in carbon dioxide at room temperature. For example, at 5wt%, the cloud point pressure for Fluorolink B was 25 MPa. Apart from that, the existence of $CO_2$-phobic aromatic groups in the fluorolink B diisocyanate prepolymer may further decrease the product solubility in carbon dioxide.

Based on the fact that most fluorinated aspartate bisureas showed poor carbon dioxide solubility, we synthesized fluorinated asparate ureas, reducing the number of $CO_2$-phobic urea functionality from two to one. Generally, the ureas exhibited enhanced solubility in carbon dioxide as we expected (compare Table 6. and Table 7.). Hexyl urea was able to dissolve in carbon dioxide at room temperature below 20 MPa, whereas 1,6-hexyl bisurea had to be heated to 90 $^0$C to dissolve at 41.4 MPa (6,000 psi).

The apparently different solubility of ureas with different R groups followed the trend of different degrees of carbon dioxide phobicity. The phenyl urea showed poor carbon dioxide solubility due to the existence of $CO_2$-phobic aryl group. The incorporation of a fluorine atom or a $CF_3$ group at the *para*-position did not enhance the solubility of the corresponding urea. The incorporation of two $CF_3$ groups at the 3,5 position, however, significantly enhanced the urea solubility in carbon dioxide. This again proved that fluoroalkyl (in this case fluoromethyl) groups are indeed $CO_2$-philic, and the

introduction of "enough" number of such $CO_2$-philic functionality could make the molecule as a whole more $CO_2$-philic.

The solubility data for fluoroalkyl ureas in carbon dioxide also revealed the same trend of relative $CO_2$-phobicity as for fluoroalkyl bisureas. That is, the aryl groups are more $CO_2$-phobic than the alkyl groups, making the hexyl urea much more soluble than the phenyl urea. We also discovered that the ethyl methacrylate, among others, was the least $CO_2$-phobic. In effect, the acrylate functionality was believed by some researchers to be $CO_2$-philic and may have favorable specific interactions with carbon dioxide.

The fluoroether was again proved to be more efficient than fluoroalkyl functionality in enhancing the urea solubility in carbon dioxide. In other words, the fluoroether was believed to be more $CO_2$-philic. The phase behavior data showed that the fluoroether ureas that we evaluated were miscible with carbon dioxide up to 5wt% at room temperature and a pressure slightly higher than the critical pressure of $CO_2$.

## 6.3. Viscosity Enhancement by Fluorinated Aspartate Bisureas and Ureas

### 6.3.1. Experimental

The experimental set-up and mechanism for solution relative viscosity measurements were described in Chapter 4.3.1. In our series of fluorinated bisureas and ureas, only those that were soluble in carbon dioxide at room temperature were subsequently evaluated for their viscosity enhancement ability.

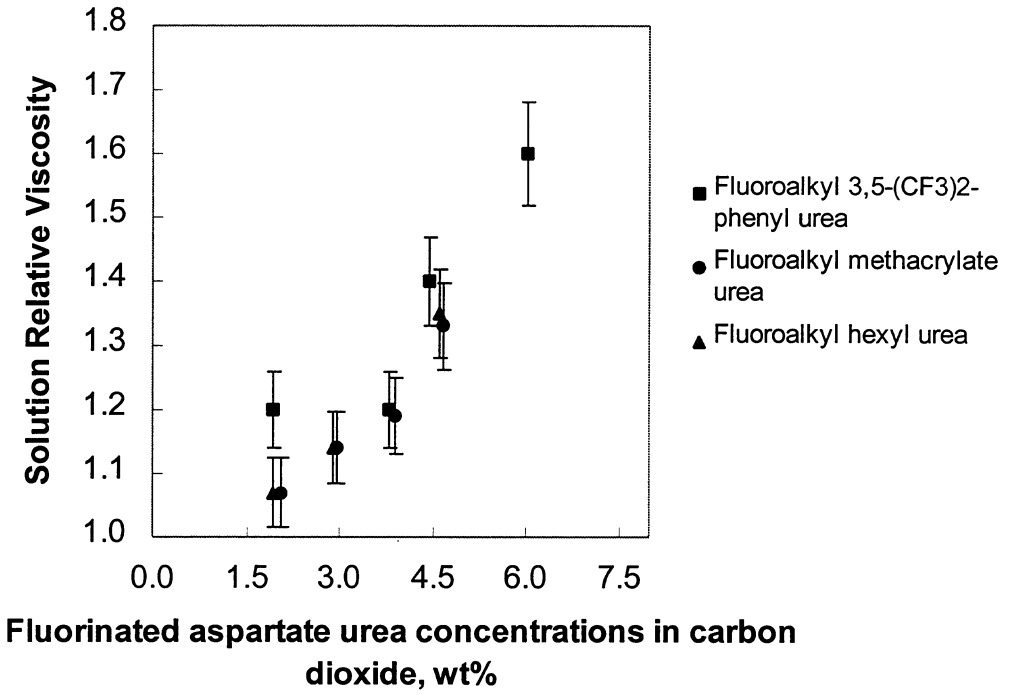


Fig.3. Solution relative viscosity of bisurea/urea in carbon dioxide,

T=298 K, P=5000 psi

### 6.3.2. Results and Discussions

The solution relative viscosity was presented in Fig. 3. Of the $CO_2$-soluble bisureas and ureas, fluoroether bisurea and ureas did not exhibit significant viscosity enhancement as detected by our high pressure falling cylinder viscometer. Or rather, the solution viscosity was almost the same as neat carbon dioxide at the same temperature and pressure. The solution viscosity for $CO_2$-soluble fluoroalkyl ureas was measured at 5,000 psi to ensure solubility of all three samples.

Overall, the fluoroalkyl ureas exhibited better viscosity enhancing capabilities than the fluoroether versions at low concentrations (< 6wt%). This is probably because the concentration of hydrogen bonding urea functionality in the fluoroalkyl version was higher than the fluoroether version owing to the much shorter fluoroalkyl group. For this reason, the fluoroalkyl ureas may have a greater chance to associate through intermolecular hydrogen bonding, leading to greater solution viscosity.

Among the three fluoroalkyl ureas, 3,5-$(CF_3)_2$-phenyl urea gave the highest solution viscosity increase, followed by hexyl urea, and the ethyl methacrylate urea gave the lowest. A possible reason for the observed greater solution viscosity for 3,5-$(CF_3)_2$-phenyl urea may be attributed to the enhanced intermolecular association through $\pi$-$\pi$ stacking of the $CO_2$-phobic phenyl rings. The relatively longer hydrocarbon chain in a hexyl urea molecule may be another factor that leads to solution viscosity increase by

intermolecular association. The long hydrocarbon chain was $CO_2$-phobic, and may promote intermolecular association through Van der Waals interactions in a carbon dioxide environment. This result proved the importance of long chain associations apart from hydrogen bonding in network formation and was consistent with the findings with similar organic solvent gelling agents.

## 6.4. Microcellular Foam Generation with Fluorinated Aspartate Bisureas and Ureas in Carbon Dioxide

### 6.4.1. Experimental

The microcellular foamed materials were generated in the same high pressure windowed cell that was used for phase behavior evaluation as described in Chapter 4.2.1. *These foams were formed using the same compounds evaluated as thickeners. Although these foams are not relevant to the study of carbon dioxide thickening agents, they do represent a novel means of generating high porosity, microcellular rigid foams.*

For the fluorinated aspartate bisureas and ureas samples that were dissolved in carbon dioxide at elevated temperatures, after a single phase solution was reached, the system was

(1) first cooled down to room temperature by blowing cold air into the air bath and turning on the cooling water in the cooling coils. At the same time, the system

pressure was kept at 6,000psi ± 100psi during cooling. The behavior was recorded before depressurization.

(2) The system pressure was subsequently decreased to the vapor pressure of carbon dioxide at room temperature. Carbon dioxide was allowed to vaporize while the pressure was reduced slowly to atmosphere pressure. The behavior was again monitored.

(3) The network samples were characterized by Scanning Electron Microscopy (SEM). Typically, the samples were first fractured in liquid nitrogen. The sample pieces were then mounted on stubs using carbon paint and sputter coated with palladium. Micrographs were taken over a range of magnifications (25x~5000x).

(4) Bulk densities for the foamed materials were evaluated simply by dividing the sample mass by its volume. Because the obtained foams were fragile samples, their volumes were not evaluated by water exclusion method. Instead, for the monolith foam, the high pressure sample cell volume was taken as the sample volume; for the collapsed foamed network, a cathometer was used to measure the height of the expanded materials. The sample volume was subsequently calculated geometrically to an approximation by treating the sample as a perfect cylinder.

(5) The appropriate depressurization rate for foamed network generation was investigated with ethyl methacrylate urea as an example because it was soluble in liquid carbon dioxide at room temperature. In a fast depressurization procedure, carbon dioxide was vented rapidly from 34.5 MPa (5,000 psi) directly to atmosphere pressure. In a slow depressurization procedure, the system pressure was first decreased to carbon dioxide

vapor pressure, and then vented slowly over more than 5 min time span. The obtained samples were characterized with SEM as described above.

(6) With hexyl bisurea as an example, the system was first heated and pressurized to obtain a single-phase solution in carbon dioxide. Then the system pressure was slowly decreased and carbon dioxide was vented while keeping the temperature at $90^0$C. The obtained sample was examined by SEM as described above.

For the samples that were soluble at room temperature, cooling is not necessary, therefore only the second and third steps were followed. If the sample can form a monolith from its carbon dioxide solution, A lower concentration was subsequently used in the experiment and the network characteristics were examined in the same way as described above.

### 6.4.2. Results and Discussions

The behaviors of the fluorinated aspartate bisureas and ureas that can form a network from their respective carbon dioxide solution were summerized in Table 5a and 5b respectively. The figure numbers for their SEM pictures were also listed in the Table. By examination, only bisureas and ureas with fluoroalkyl side chains were able to generate network structures from carbon dioxide solution. Therefore only the R groups ($CO_2$-"phobic" groups) were specified in the Tables.

| R group | concentration | cooling | depressurization | Fig. # | density, $g/cm^3$ |
|---|---|---|---|---|---|
| $(CH_2)_6$ | 3.0-4.9wt% | I | I | 19a | 0.026 |
| | 2.2wt% | II | II | 19b | 0.19 |
| $(CH_2)_{12}$ | 4.0wt% | II | II | 20 | 0.51 |

Table 5a. Network formation from carbon dioxide solution of fluorinated aspartate bisureas

| R group | concentration | cooling | depressurization | Fig. # | density, $g/cm^3$ |
|---|---|---|---|---|---|
| *p*-F-phenyl | 4.5wt% | II | II | 21 | 0.88 |
| 3,5-$(CF_3)_2$-phenyl | 2.0-6.0wt% | ---- | II | 22 | 0.075 |
| $CH_3(CH_2)_5$ | 3.7-5.0wt% | ---- | II | 23 | 0.06 |
| phenyl | 4.8-5.1wt% | I | I | 24a | 0.045 |
| | 1.5wt% | II | II | 24b | 0.044 |
| ethyl methacrylate | 4.7wt% | ---- | II | 25 | 0.080 |

Table 5b. Network formation from carbon dioxide solution of fluorinated aspartate ureas

I. a network that filled the whole sample cell;

II. a collapsed network that filled part of the sample cell.

## 7.0 Fluoroacrylate-Styrene Copolymers

### 7.1 Introduction

To enhance the viscosity of carbon dioxide by the factor needed (2-100), agents should create the thermodynamic illusion of very high molecular weight via non-covalent association. It has been reported[24, 25] that random, lightly sulfonated polystyrene can greatly increase solution viscosity in non-polar organic solvents through the association of the acid or salt groups in the polymeric chain. Unfortunately, polystyrene does not dissolve in dense carbon dioxide at reasonable pressures and temperatures. In this paper, we report that highly $CO_2$-soluble styrene/fluorinated acrylate copolymers can enhance the viscosity of $CO_2$ by factors greater than 100, at concentrations less than 5 wt %. When these associating polymers are employed in dense carbon dioxide at low concentration (less than 5 wt %), we have observed the 2 order of magnitude increase in viscosity necessary to conduct $CO_2$-based enhanced oil recovery without "fingering". Lightly sulfonated copolymers were also synthesized, and falling cylinder viscometry results showed that they also exhibited enhanced thickening behavior in neat dense carbon dioxide, although they exhibit lower solubility in carbon dioxide than unsulfonated analogs.

### 7.2 Experimental

**Materials.** Styrene was purchased from Aldrich and was distilled under vacuum before use. 3,3,4,4,5,5,6,6,7,7,8,8,9,9,10,10,10-heptadecafluorodecyl acrylate (HFDA) was

obtained from Aldrich and was purified in order to remove inhibitor before use. All other reagents and solvents were received from Aldrich and were used without further purification unless otherwise indicated.

**General Procedures.** Copolymers from HFDA and styrene monomers were obtained by bulk free radical polymerization using AIBN as initiator (Scheme 1). Under an inert $N_2$ atmosphere, a 50 mL glass ampule was charged with 5.18g monomer HFDA (0.01 mol), 0.42g styrene (4.0 mmol) and 4.6mg AIBN. The ampule was sealed and placed in a water bath at 65 °C for 12 hours. The reaction mixture was cooled, then dissolved in 1,1,2-trichlorotrifluoroethane. The polymer was precipitated in methanol, washed, and dried under reduced pressure. Copolymers were lightly sulfonated at 50 °C in 1,1,2-trichlorotrifluoroethane using acetyl sulfate according to the procedure of Makowski et al[27].

Fourier transform infrared spectroscopy (FTIR) measurements were performed on a Mattson FTIR using KBr disks at a resolution of 4 $cm^{-1}$. $^1H$ NMR was recorded on a Bruker 300M NMR instrument. Intrinsic viscosities of the polymers were determined in 1,1,2-trifluorotrichloroethane at 25 °C using an Ubbelohde viscometer.

**Phase behavior and viscosity measurements.** The phase behavior and viscosity measurements were performed at room temperature using a high pressure, variable-volume, windowed cell as shown in Scheme 2. Isothermal compressions and expansions of mixtures of specified overall composition were used to initiate phase separation. Visual observations of the initial appearance of a second phase (cloud points or bubble points) indicated location of the phase boundary.

The viscosity of single-phase polymer-$CO_2$ solutions was determined by falling cylinder viscometry. This technique was selected because of its simplicity in monitoring large viscosity increases in fluids as indicated by reductions in the terminal velocity ($u_t$) of a falling object:

$$\eta_f = \frac{K(\rho_s - \rho_l)}{\mu_t} \qquad (1)$$

where K is the calibration constant, $\rho_s$ is the solid cylinder density, $\rho_l$ is the liquid carbon dioxide density, and $\eta_f$ is the fluid viscosity. Although other viscosity measurements, (e.g. capillary viscometry and pressure drop through porous media) provide more comprehensive and precise assessments of viscosity as a function of shear rate, falling object (ball, sphere, cylinder, needle) viscometry remains a simple technique that rapidly provides an indication of significant viscosity changes.

The viscosity tests were performed using the phase behavior apparatus. As shown in Scheme 3, a finely machined aluminum cylinder was placed in the cylindrical sample volume before the polymer sample and the mixing balls were added. After equilibration of the system, the cell was rapidly inverted and the terminal velocity of the cylinder was measured. The falling aluminum cylinder viscometer was calibrated using neat carbon dioxide. Changes in the solution density relative to that of neat carbon dioxide were assumed to be small relative to the density difference between aluminum and carbon dioxide, and thus the relative viscosity (solution viscosity/viscosity of neat carbon dioxide) was equivalent to the terminal velocity ratio (terminal velocity in neat carbon

dioxide/terminal velocity in solution). Terminal velocities were determined by dividing the length of the cylinder's fall by the duration of the fall. The experiment was repeated 5 times at each concentration, and the average relative viscosity results were reported.

## 7.3 Results and discussion

Copolymers of styrene and the fluoroacrylate were characterized using $^{1}H$ NMR and intrinsic viscosity in 1,1,2-trichlorotrifluoroethane (TCTFE). Results are reported in Table1.

**Phase behavior of polymers in liquid carbon dioxide.** Although carbon dioxide, in both its liquid and supercritical states, is miscible with many small molecules, it is a relatively poor solvent at easily accessible conditions (temperature <100 °C and pressure <50 MPa). Materials that exhibit low or negligible solubility in pure carbon dioxide include most polymers (except amorphous or low-melting fluoropolymers and silicones), waxes, heavy oils, proteins, salts, and metal oxides. It has been reported[21] in our laboratory that the homopolymer of HFDA is soluble in liquid carbon dioxide at concentration of up to 5 wt % at room temperature and low pressure (below 10 MPa). DeSimone and co-workers[21] have reported on the high solubility of poly(1,2-dihydroperfluorooctyl acrylate) (polyFOA) in supercritical carbon dioxide at low pressure as well.

Figure 1 shows that the experimental cloud point curves of PHFDA-xPSt copolymers in carbon dioxide at 25 °C with concentration varying from 1.0 to 5.0 wt %. Not surprisingly, the copolymer becomes more difficult to dissolve in carbon dioxide as

styrene content increases, because styrene repeat units are known to be $CO_2$-phobic. When the styrene content reaches 40 mole %, concentrations of more that 3 wt %, copolymer do not completely dissolve in carbon dioxide at 25 °C below 50 MPa. It should be noted that the polymers shown in Table 1 exhibit differences in molecular weight (as shown by intrinsic viscosity) as well as styrene content. Ordinarily, the cloud point pressure increases sharply as polymer molecular weight increases, and thus the data in Figure 1 reflect both molecular weight and styrene content variations. However, if we compare the clould point curves that represent the two copolymers with identical styrene content (29 mole %) and different molecular weight (intrinsic viscosity of 175 and 196, respectively), it appears that styrene content plays a more significant role than molecular weight in determining the location of the phase boundary for these copolymers. This is supported by the results for the 29% and 33% styrene copolymers; the miscibility pressures for the 33% styrene material are significantly higher, despite the fact that this material exhibits a lower molecular weight.

The neutralized sulfonated copolymer (NSC) is more difficult to dissolve in carbon dioxide than its unsulfonated analog because the high-polarity salt is more $CO_2$-phobic. Figure 2 shows the cloud points of NSC (PHFDA-0.22PSt-0.027S) in carbon dioxide vs. concentration. Compare to its unsulfonated analog (PHFDA-0.22PSt), it exhibits much higher cloud point pressures, especially at high concentration.

**Viscosity behavior of the polymers.** In an earlier attempt to raise the viscosity of liquid carbon dioxide, we synthesized and evaluated telechelic (sulfonate-teminated) fluorinated polyurethanes, polymers that may undergo association in solution. The relative viscosity approached 3 at concentrations of 5 weight percent polymer, a

significant enhancement but far short of what would be necessary to effectively practice $CO_2$-based enhanced oil recovery (EOR). Hence, we evaluated materials with others means for association in solution. It is known that phenyl groups can "stack" in organic solvent[28]; association from the stacking of phenyl groups in our copolymers would provide a fundamental force to raise the viscosity of the solution. Figure 3 illustrates the viscosity behavior of the copolymers in liquid carbon dioxide with concentrations varying from 1 wt % to 5 wt % at 25 °C and 34.48 MPa. All of the copolymers enhance the viscosity of neat liquid carbon dioxide, yet not to the same degree. As shown in the figure, there exists an optimum level of styrene (approximately 29 mole %) insofar as viscosity enhancement is concerned. For copolymers (PHFDA-0.29PSt) with the same composition and different molecular weight, not surprisingly, the one with higher molecular weight shows a higher extent of viscosity-enhancement. It might be expected that if $\pi$ - $\pi$ stacking is governing the viscosity enhancement of these copolymers solutions, then increasing the number of phenyl groups (increasing the styrene content) would produce a monotonic increase in the viscosity, rather than the behavior shown in Figure 3. However, the phase behavior results show that increasing the styrene content in the copolymers renders the polymer-solvent thermodynamics less favorable ($CO_2$ is a poorer solvent for copolymers with higher styrene contents). Hence, the polymer coils will not be as expanded in solution at higher styrene contents, potentially leading to fewer inter-chain associations and a larger number of intra-chain associations.

We surmise that $\pi$ - $\pi$ stacking between phenyl groups is contributing to the strong viscosity enhancement effect of the copolymers, because copolymers lacking the aromatic

group produce a much lower degree of viscosity enhancement in carbon dioxide. We synthesized copolymers, for example, from the fluorinated acrylate and hydrocarbon acrylates (N,N-dimethylamino ethyl acrylate (DMAEA) and hexyl acrylate (HA), respectively). Experimental results show that these polymers do not exhibit significant viscosity enhancement in neat liquid carbon dioxide, as shown in Figure 4.

Not surprisingly, the solution viscosity increases as pressure increases. Figure 5 shows the viscosity behavior of the copolymer (PHFDA-0.29PSt) in carbon dioxide at concentrations varying from 1 to 5 wt % and pressures from 20.69 MPa to 41.38 MPa. It is known that increasing pressure will increase the viscosity of pure $CO_2$ (viscosity is a function of fluid density), but this dependence is already accounted for because the data in Figure 5 are reported as relative viscosities. However, solution viscosity could be a strong function of polymer volume fraction, given by:

$$\phi_p = \frac{1}{1 + \frac{\rho_p}{\rho_c}\left(\frac{1-\omega}{\omega}\right)}$$

where the ρ's are the density of the polymer and $CO_2$, and w is the weight fraction polymer. Hence, as pressure increases, the volume fraction of polymer increases even though the weight fraction remains constant, given that $CO_2$ is much more compressible than the polymer. However, even this adjustment would not account for the large relative viscosity increase with increasing pressure. The pressure-induced increase in viscosity enhancement shown in Figure 5 may derive from the fact that $CO_2$ is a better solvent at

higher pressures, and thus the polymer coils will be more expanded in solution at higher pressures. Greater coil expansion could lead to higher viscosity through larger numbers of inter-chain association points.

Just as lightly sulfonated polystyrene exhibits viscosity-thickening behavior in conventional organic solvents, the neutralized lightly sulfonated copolymers from styrene and fluorinated acrylate were found to significantly enhance the solution viscosity in neat liquid carbon dioxide. Figure 6 shows the viscosity behavior of a neutralized lightly sulfonated copolymer (PHFDA-0.22PSt-0.027S) and its unsulfonated analog (PHFDA-0.22PSt) in carbon dioxide at concentrations from 1 to 4 wt % at 34.48 MPa and 25 °C. The neutralized lightly sulfonated copolymer can increase the viscosity to a higher extent than its unsulfonated analog due to ionic association in solution. Unfortunately, the neutralized lightly sulfonated copolymer is more difficult to dissolve in carbon dioxide at reasonable conditions.

**Shear rate effect on the relative viscosity**. We have also found that the associating styrene-fluoroacrylate copolymers exhibit shear-thinning behavior in carbon dioxide. We have assumed that these polymers belong to the first class of the three general classes of non-Newtonian fluids[29]: those whose properties are independent of time or duration of shear.

In time-independent materials, most polymeric solutions are pesudoplastic, where the apparent viscosity decreases with increasing shear rate. Eichstadt and co-workers[30] have previously reported the development of the theoretical description of the behavior of the falling cylinder viscometer for time-independent, non-Newtonian solutions. In the polymer-$CO_2$ solution system we can measure the relative viscosity of the solution using

equation 1. However, it should be noted that the shear rate is a function of the absolute speed with which the cylinder falls during the measurement. Consequently, the shear rates that we can attain in the device are themselves a function of the concentration of any given solution, as the polymer concentration determines the speed at which the cylinder falls (and hence the relative viscosity). For a control volume in the annular gap between the cylinder and the wall, the equation of motion in the z direction gives[31, 32]:

$$\rho\left(\frac{\partial U_z}{\partial t}+U_r\frac{\partial U_z}{\partial r}+U_\theta\frac{\partial U_z}{\partial \theta}+U_z\frac{\partial U_z}{\partial z}\right)=\frac{dp}{dz}+\eta\left(\frac{1}{r}\frac{\partial}{\partial r}\left(r\frac{\partial U_z}{\partial r}\right)+\frac{1}{r^2}\left(\frac{\partial^2 U_z}{\partial \theta^2}\right)+\frac{\partial^2 U_z}{\partial z^2}\right)+\rho g z \quad (2)$$

Where $Ur$, $U_\theta$, $Uz$ are the fluid velocities in $r$, $\theta$, $z$ directions, $\rho$ is density, $p$ is the pressure, and t is time. Because the solution is time independent, $\frac{\partial Uz}{\partial t}=0$. Further, $\frac{\partial Uz}{\partial \theta}$ and $\frac{\partial Uz}{\partial z}$ vanish because the velocity in the z direction doesn't vary in the $\theta$ or $z$ directions.

The boundary conditions are:

$$Uz = 0, \qquad @r = r_t \qquad (3)$$

$$Uz = U_t \qquad @r = r_c \qquad (4)$$

Where $r_t$ is the inside radius of the glass tube, $r_c$ is the radius of the aluminum cylinder, and $r$ is the distance from the central line of the cylinder.

Solving the differential equation (2) with the boundary conditions [(3) and (4)], we can derive the shear rate,

$$Shear\ Rate = \frac{dUz}{dr} = U_t.\left[\frac{-2r_c - (r_t^2 - r_c^2)\dfrac{1}{r_c \ln(r_c/r_t)}}{r_t^2 - r_c^2 + \ln(r_c/r_t)(r_t^2 + r_c^2)} + \frac{1}{r_c \ln(r_c/r_t)}\right] \qquad (5)$$

where $U_t$ is the cylinder terminal velocity in the $z$ direction.

Equation (5) shows that the shear rate will vary as either the terminal velocity or the radius of the falling cylinder changes. Consequently, we performed a series of experiments on the polyfluoroacrylate-co-polystyrene (29% styrene) where either the polymer concentration or the aluminum cylinder radius were varied (note that each of these will affect the terminal velocity). Consequently, we could evaluate the effect of shear rate (defined by equation (5)) on the viscosity, as shown in Figure 7. From this data we conclude that these copolymer/CO2 solutions are shear thinning, a useful attribute in enhanced oil recovery.

A more complete study of the falling cylinder viscometry analysis of this system, including aditional viscosity data, is presented in the appendix.

## 7.4 **Conclusion**

Highly $CO_2$ soluble copolymers from perfluoroacrylate and styrene monomers were synthesized by free radical polymerization. Cloud point experiments indicate that the solubility of the polymers decreases with increasing styrene content in the polymer chain. A neutralized, lightly sulfonated polymer was also obtained, and it was more difficult to dissolve in liquid carbon dioxide than its unsulfonated analog because of ionic association in the solution. All of these copolymers can enhance the viscosity of carbon dioxide by several orders of magnitude at relatively low concentration at room temperature, possibly because of "stacking" structure of phenyl groups in the solution. In addition, an optimum level of styrene (approximately 29 mole %) with regards to viscosity-thickening behavior in carbon dioxide was observed. The study of shear rate effect on viscosity behavior of polymer- $CO_2$ solution shows that the relative viscosity decreases as shear rate increases. We are actively investigating changes to molecule structure of the polymer that will provide high viscosity-thickening behavior in carbon dioxide at low concentration (<1 wt %), and reduction in the weight percent fluorine in the associating molecules or replacement of fluorine with new, less expensive $CO_2$-philic groups.

## 7.5 References


1. McHugh, M. A.; Krukonis, V. J. *Supercritical Fluid Extraction Principles and Practice*; Butterworth: Stoneham, MA, 1994.
2. Garg, A.; Gulari, E.; Manke, C. W. *Macromolecules* **1994**, 27, 5643.
3. Shi, C.; Huang, Z.; Kilic, S.; Xu, J.; Enick, R. M.; Beckman, E. J.; Carr, A. J.; Melendez, R. E.; Hamilton, A. D. *Science* **1999**, 286 (5444), 1540.
4. DeSimone, J. M.; Maury E. E.; Menceloglu, Y. Z.; McClain, J. B.; Romack, T. J.; Combes, J. R. *Science* **1994**, 265, 356.
5. Adamsky, F. A.; Beckman, E. J. *Macromolecules* **1994**, 27, 312.
6. Dillow, A. K.; Yun, S. L.; Suleiman, D. S.; Boatright, D. L.; Liotta, C. L.; Eckert, C. A. *Ind. Eng. Chem. Res.* **1996**, 35, 1801.
7. Johnston, K. P.; Harrison, K. L.; Clarke, M. J.; Howdle, S. M.; Heitz, M. P.; Bright, F. V.; Carlier, C.; Randolph, T.W. *Science* **1996**, 271, 624.
8. Mesiano, A. J.; Beckman, E. J.; Russell, A.J. *Chem. Rev.* **1999**, 99, 623.
9. Lemert, R. M.; Johnston, K. P. *Ind. Eng. Chem. Res.* **1991**, 30, 1222.
10. Hoefling, T. A.; Beitle, R. R.; Enick, R. M.; Beckman, E. J. *Fluid Phase Equilibr.* **1993**, 83, 203.
11. Stalkup, F. I. *SPE Monograph*, No. 8, New York, NY, 1983.
12. Enick, R. M.; Iezzi, A.; Bendale, P.; Brady, J. *Fluid Phase Equilibr.* **1989**, 53, 307.
13. Heller, J. P.; Dange, D. K. *SPE J.* **1985**, 25(5), 675.
14. Iezzi, A. M. S. Thesis, University of Pittsburgh, 1989.

15. Gullapalli, P.; Tsau, J. S.; Heller, J. P. *SPE 28979, presented at SPE International Symposium on Oilfield Chemistry*, San Antonio, TX, Feb. 14-17, 1995.

16. Davis, B. U.S. Patent, 4,989,674, 1991.

17. Llave, F.; Chung, F.; Burchfield, T. *SPE RE* **Feb. 1990**, 47-51.

18. DeSimone, J. M.; Guan, Z.; Elsbernd, C. S. *Science* **1992**, 257, 945.

19. McClain, J. B.; Betts, D. E.; Canelas, D. A.; Samulski, E. T.; DeSimone, J. M.; Londono, J. D.; Cochran, H. D.; Wignall, G. D.; Chillura-Martino, D.; Triolo, R. *Science* **1996**, 274, 2049.

20. Canelas, D. A.; Betts, D. E.; DeSimone, J. M. *Macromolecules* **1996**, 29, 2818.

21. McClain, J. B.; Betts, D. E.; Canelas, D. A.; Samulski, E. T.; DeSimone, J. M.; Londono, J. D.; Wignall, G. D. *Polym. Mater. Sci. Eng.* **1996**, 74, 234.

22. Enick, R. M.; Beckman, E. J.; Shi, C.; Karmana, E. *J. Supercritical Fluid* **1998**, 13, 127.

23. Shi, C.; Beckman, E. J.; Enick, R. M. Submitted to Macromolecules.

24. Agarwal, P. K.; Lundberg, R. D. *Macromolecules* **1984**, 17, 1918.

25. Chakrabarty, K.; Shao, L. Y.; Weiss, R. A. In *Ionomers: Synthesis, Structure, Properties and Applications*; Tant, M. R.; Mauritz, K. A.; Wilkes, G. L. Eds.; Chapman and Hall: London, 1997; p158.

26. Otsu, T.; Matsumoto, A.; Tazaki, T. *Polym. Bull.* **1987**, 17, 323.

27. Makowski, H. S.; Lundberg, R. D.; Singhal, G. H. U.S. Patent, 3,870,841, 1975.

28. Tata, M.; John, V. T.; Waguespack, Y. Y.; McPherson, G. L. *J. Am. Chem. Soc.* **1994**, 116, 9464.

29. Perry, R. H.; Chilton, C. H. *Chemical Engineering handbook*, fifth edition, McGraw-Hill, New York, 1973, p5-38.

30. Eichstadt, F. J.; Swift, G. W. *A.I.Ch.E Journal* **1966**, 12, 2279.

31. Rouse, H.; Ince, S. *History of Hydraulics*, Iowa Institute of Hydraulics, Iowa City, 1959.

32. Bird, R. B.; Stewart, W. E.; Lightfoot, E. N. *Transport Phenomena*, John Wiley & Sons, Inc., New York, 1960, p10.

Table 1. Composition of copolymers

| Polymer [a] | Content of Polystyrene (mol.%) | | Intrinsic viscosity [c] (g/mL) |
|---|---|---|---|
| | Theoretical | By $^1$HNMR | |
| PHFDA-0.22PSt | 0.22 | 0.258 | 117.8 |
| PHFDA-0.25PSt | 0.25 | 0.273 | / |
| PHFDA-0.29PSt | 0.29 | 0.292 | 175.4 |
| PHFDA-0.29PSt(II) [b] | 0.25 | 0.299 | 196.4 |
| PHFDA-0.33PSt | 0.33 | 0.347 | 145.8 |
| PHFDA-0.40PSt | 0.40 | 0.403 | / |

[a] Polymerization conditions: [AIBN]/[monomers] = 0.2 mole %, 60 °C, 24 hours.
[b] This polymer was synthesized by bulk polymerization using 2,3-dicyano-2,3-diphenyl-succinic acid diethyl ester as initiator[26]. Reaction conditions: [initiator]/[monomers] = 0.05 mole %, 70 °C, 4 days.
[c] Intrinsic viscosity was determined in 1,1,2-trichlorotrifluoroethane at 25 °C.

Scheme 1.

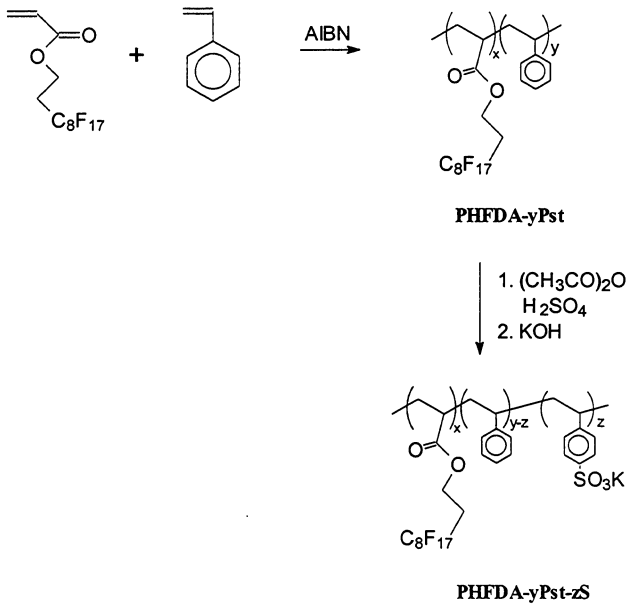

Scheme 2.

High Pressure, Variable Volume, Windowed Cell (D. B. Robinson Cell)

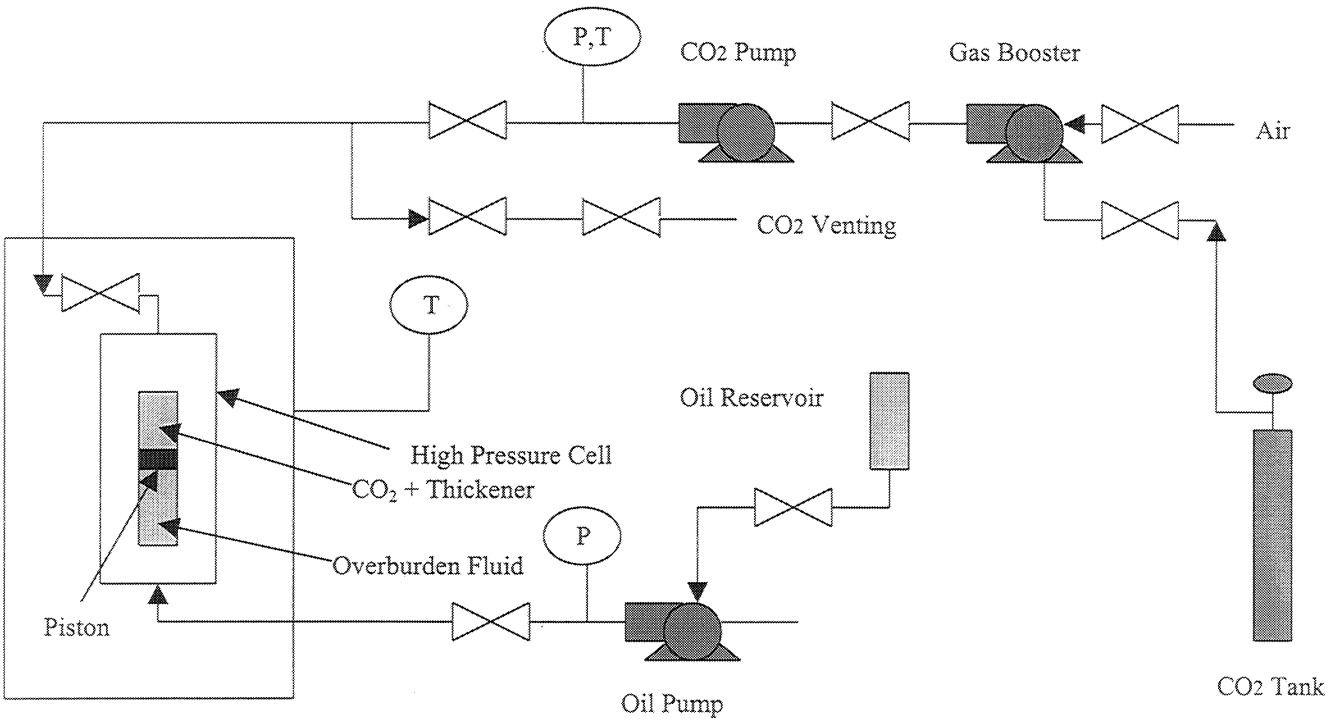

Scheme 3.

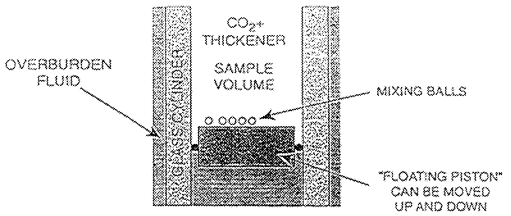


SOLUBILITY ARRANGEMENT

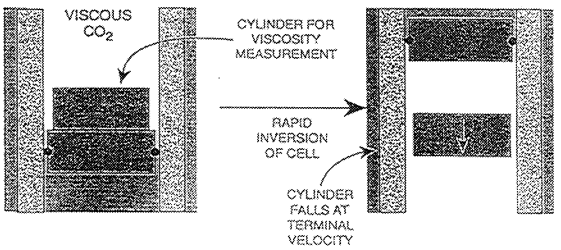


VISCOSITY MEASUREMENT

Figure 1. Experimental results of Poly(HFDA)-Polystyrene copolymers cloud point behavior in $CO_2$ at 25 °C.

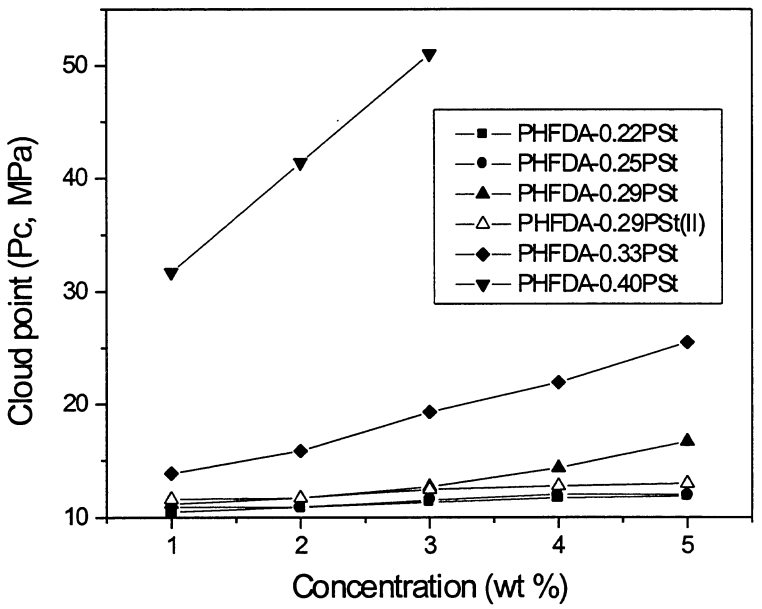

Figure 2. Cloud point result of the neutralized lightly sulfonated copolymer (PHFDA-0.22PSt-0.027S) in $CO_2$ at 25 °C.

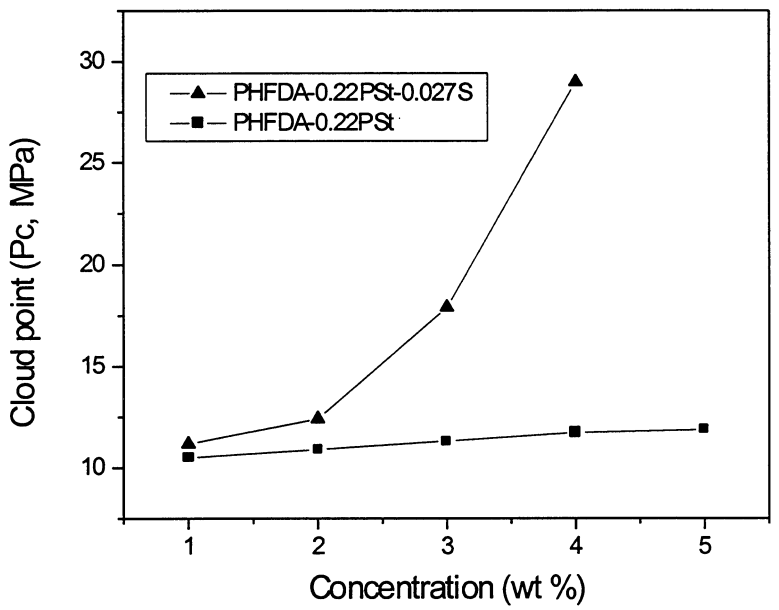

Figure 3. Relative viscosity of copolymer solutions in $CO_2$ as a function of concentration at pressure of 34.48 MPa and 25 °C.

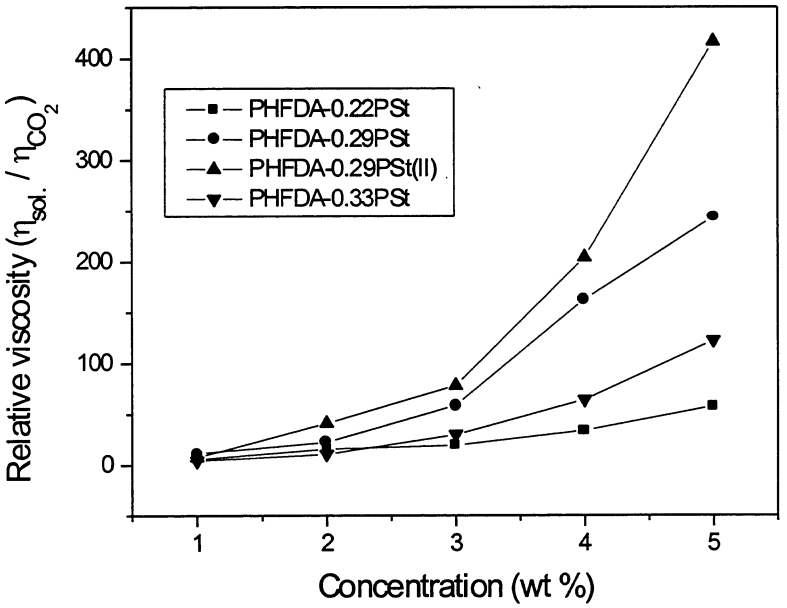

Figure 4. Relative viscosity of $CO_2$-polymer solutions as a function of polymer type and concentration at pressure of 34.48 MPa and 25 °C. PHA: Poly(hexyl acrylate); PDMAEA: Poly(2-dimethylamino ethyl acrylate).

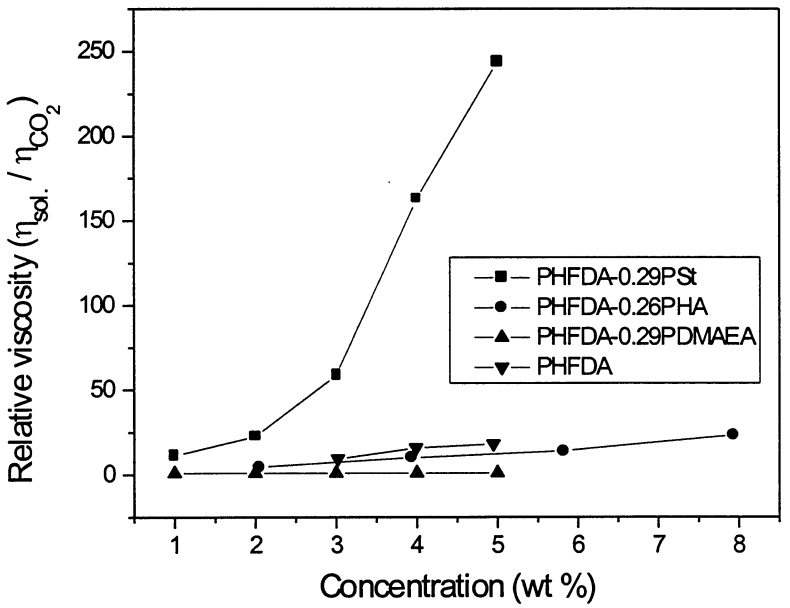

Figure 5. Relative viscosity of copolymer PHFDA-0.29PSt solution in $CO_2$ as a function of concentration at pressure varying from 20.69 to 41.38 MPa and 25 °C.

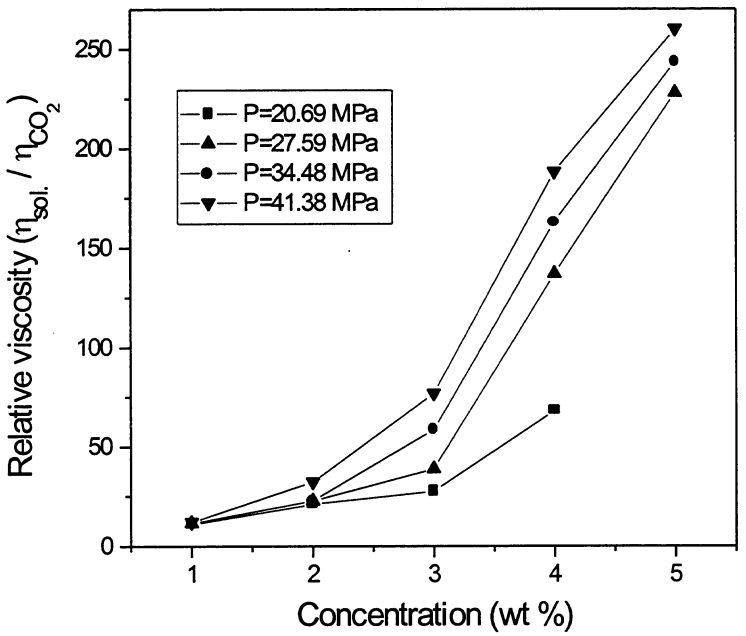

Figure 6. Relative viscosity of solutions of copolymer PHFDA-0.22PSt and its neutralized lightly sulfonated polymer PHFDA-0.22PSt-0.027S in $CO_2$ as a function of concentration at pressure of 34.48 MPa and 25 °C.

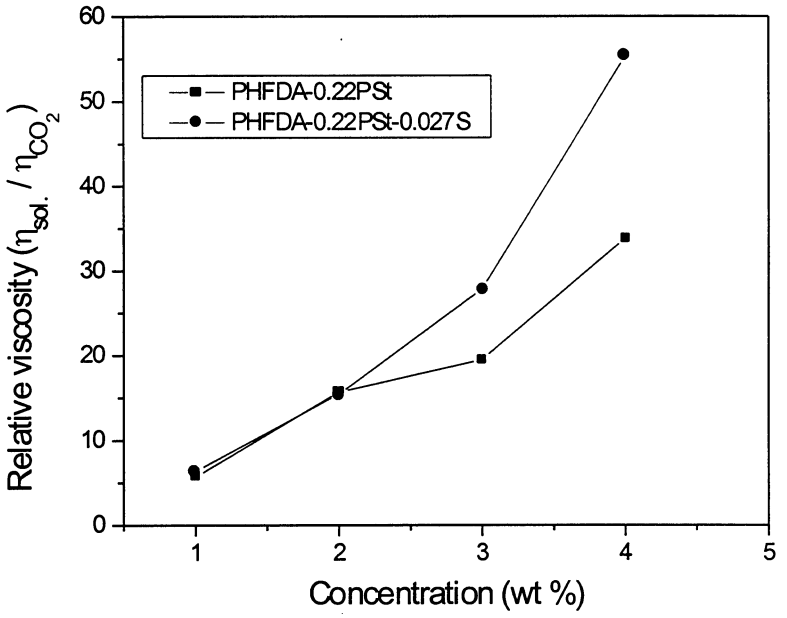

Figure 7. Relative viscosity of copolymer PHFDA-0.29PSt solution in $CO_2$ as a function of shear rate at pressure of 34.48 MPa and 25 °C.

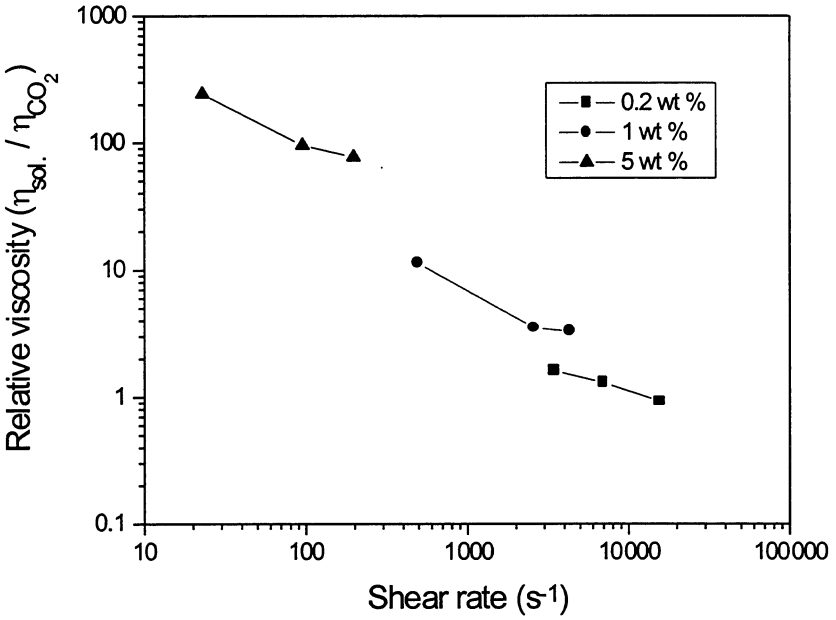

# 8.0 Sulfonated Fluoroacrylate-Styrene Copolymers

## 8.1 Introduction

It was ascertained in our group earlier that homopolymers of fluoropolymers do not exhibit substantial increase in viscosity although they are soluble at reasonable pressure and moderate temperature. This situation necessitated incorporation of another groups to the backbone of polymers. Therefore, in our group we synthesize copolymers of fluoroacrylate monomer with various $CO_2$-phobic monomers which have special chemical and/or physical interactions with $CO_2$ or within the polymer to contribute viscosity enhancement. These include aromatic groups, as illustrated in the previous section, and sulfonte groups. These polar sulfonate groups can lead to intermolecular ionic associations similar to those described in the previous section on ionic associations of fluoroether disulfates.

## 8.2 Experimental

### 8.2.1. Synthesis of Random Copolymer of Hexyl acrylate with Fluoroacrylate:

*8.2.1.1. Material*

3,3,4,4,5,5,6,6,7,7,8,8,9,9,10,10,10,10-heptadecafluorodecyl acrylate monomer (97%) and Hexyl acrylate (98%) were obtained from Aldrich, and both monomers were purified before use in order to remove inhibitors. Initiator, AIBN (98%, Aldrich) was recrystallized from methanol. Solvent Freon (99.8%, 1,1,2-trichlorotrifluoroethane, Aldrich), Methanol (anhydrous, Aldrich) were used as received.

**Synthesis Procedure**

Copolymerization was carried out by bulk free radical polymerization of fluoroacrylate and hexyl acrylate in the presence of AIBN. A mixture of AIBN (approximately 0.2 mole % of monomers), hexyl acrylate and fluoroacrylate was placed in an ampule. The mixture was purged with $N_2$ and then, the ampule was sealed with flame. The reaction mixture was kept at 65-70 °C overnight. The resulted semi-transparent sticky solid polymer was transferred to Freon and precipitated into methanol. Product was purified several times by dissolution in Freon and reprecipitation in methanol. After vacuum-oven-dry overnight, copolymers were obtained with 90-95 % yield. .

## 8.2.2. Synthesis of Random Copolymer of Fluoroacrylate and Styrene with Sulfate Group

### *8.2.2.1. Material*

All reagents, except 95 % sulfuric acid and NaOH pellets (J. T. Baker), were purchased from Aldrich. Monomers (3,3,4,4,5,5,6,6,7,7,8,8,9,9,10,10,10,10-heptadecafluorodecyl acrylate and styrene) and AIBN were purified via standard procedures. Freon (1,1,2-trichlorotrifluoroethane), Methanol (anhydrous), 1,2 dichloroethane, and acetic anhydride (99+%) were used as received.

### *8.2.2.2. Synthesis Procedure*

Synthesis of random copolymer of fluoroacrylate and styrene with sulfate group follows three-step procedure:

a) *Random Copolymerization of Fluoroacrylate and Styrene*

A mixture of AIBN, styrene and fluoroacrylate was placed in an ampule. The mixture was purged with $N_2$, and then sealed with flame. A white solid (candle-like) was resulted in after overnight polymerization reaction at ~65-70 °C. Polymer was purified by dissolving in Freon and precipitating in a large excess of methanol. After vacuum oven dry overnight, a white polymer was obtained with 95% yield.

*b) Sulfonation of Copolymer of Fluoroacrylate and Styrene*

Sulfonation of phenyl group was performed using acetyl sulfate as reagent. Reagent was prepared according to the procedure reported in literature (4-6). For sulfonation, copolymer prepared in the previous step was dissolved in Freon. Solution was heated up to 50-60 °C under reflux. After adjustment of the temperature, pre-prepared acetyl sulfate solution was added. When acetyl sulfate was added to the polymer solution, solution acquired a dark green/brown tint. The reaction was allowed to proceed 2 hours at 50-60 °C and then terminated by the addition of large amount of methanol. To facilitate the complete removal of residual sulfonating agent from the functionalized polymer, the sulfonated polymer was redissolved in Freon and reprecipitated in methanol several times. Then, sample was dried in a vacuum oven overnight.

c) *Neutralization of Sulfo-functionalized Copolymer*

To the solution of sulfonated copolymer in Freon, added 4-5 drops of 1 wt % phenolphthalein (indicator). Solution was titrated by 1.0 N NaOH until the end point

indicated by a change from colorless to pink. Resulting functionalized ionomer was precipitated in methanol. Polymer was purified several times by redissolution in Freon and reprecipitation in methanol. After drying in vacuum oven overnight, slightly brown tint polymer was obtained.

### 8.2.3. Synthesis of Random Copolymers of Fluoroacrylate with Monomers Possessing Aromatic Groups

*8.2.3.1. Material*

All reagents, namely Acryloyl chloride (96%), Tetrahydrofuran (99.9%, anhydrous) Triethylamine (99.5%), phen ethyl alcohol (99+%), 1-naphthaleneethanol (98%), monomer (3,3,4,4,5,5,6,6,7,7,8,8,9,9,10,10,10,10-heptadecafluorodecyl acrylate) and initiator (AIBN), Freon (1,1,2-trichlorotrifluoroethane), Methanol (anhydrous), were purchased from Aldrich. Except AIBN (recrystallized from methanol), all chemicals were used as received.

*8.2.3.2. Synthesis Procedure*

Synthesis of random copolymers of fluoroacrylate with monomers possessing aromatic groups requires two-step procedure:

*a) Reagent preparation of monomers possessing aromatic groups*

A mixture of tetrahydrofuran (THF), alcohol, triethylamine ($Et_3N$, 30 mole % excess of alcohol) was put into three-necked round bottom flask equipped with magnetic stirrer, a

dropping funnel. The mixture was maintained at around 0 °C in an ice/water bath and under nitrogen. In the meantime, acryloyl chloride (30 mole % excess of alcohol) dissolved in THF was added in a dropwise fashion to the mixture of alcohol and triethylamine dissolved in THF. Addition lasted 1.5 hr. The resulting solution was stirred at around 0 °C for 6 hrs and left overnight at room temperature under $N_2$. Visible $Et_3.HCl$ salt was filtered off and rinsed with dichloromethane several times. Extractions were performed in the filtrate four times with 5% $NaHCO_3$, and five times with distilled water. The resultant organic layer was dried over $Na_2SO_4$ and filtered. The solution was concentrated on a rota-vapor to remove solvent and other unreacted reagents. A yield of about 55-70% was obtained.

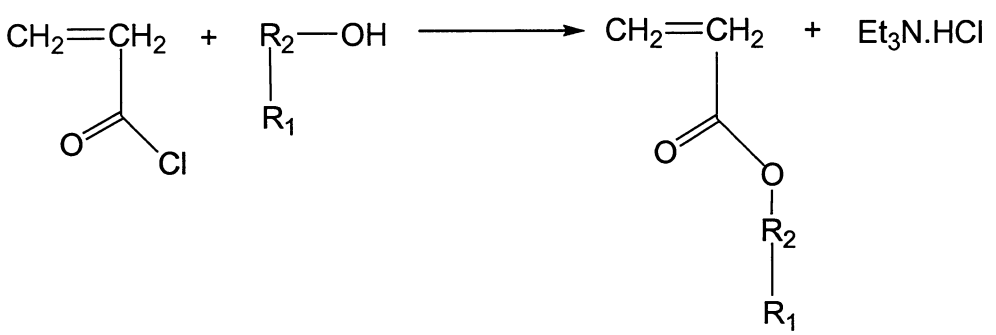


where

$R_1$: $(Ar)_x$

$R_2$: $(CH_2)_y$

*b) Polymerization of pre-prepared monomer with fluoroacrylate monomer*

Polymerization was performed according to the procedure explained above in Section 2.1.2 and 2.2.2.

## 1. Characterization

Chemical characterization of the resulting products was accomplished via 300 MHz $^1H$ NMR spectroscopy. NMR spectroscopy was carried out by dissolving sample in Freon in an 8 mm O.D. inner tube, which is then placed in an 10 mm O.D. outer tube containing deuterated chloroform and tetramethylsilane. Aromatic ring and acrylate groups were the characteristic peaks that we used for calculation of chemical composition since they give peaks in the upstream of the spectra. Chemical structures and compositions of the molecules are depicted in Table 1.

**Table 1**. Chemical structures and compositions of the molecules.

| Chemical structure | $CO_2$-philic Fraction (x) | CO2-phobic Fraction (y) | Ionic Fraction (z) |
|---|---|---|---|
| 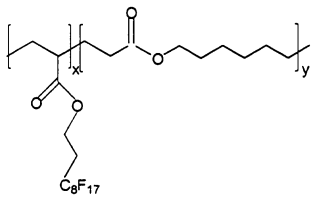 | 74 | 26 | - |
| 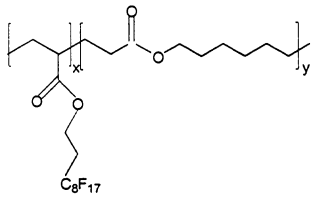 | 54 | 46 | - |

| | | | |
|---|---|---|---|
| | 86 | 16 | - |
| | 86 | 14 | 2 |
| | 86 | 11 | 5 |
| | 82 | 18 | - |

## 2. Result and Discussion

Phase behavior and viscosity measurements of copolymers were performed at room temperature using high-pressure cell with varying volume. Cloud point pressure of solution was determined as the point where the solution turned cloudy (visually) as the pressure was slowly decreased from a pressure at which solution was single phase. Viscosity measurements of the solutions were carried out using falling cylinder, and measuring falling time between two fixed points. Viscosity measurements were done only when the solution was single-phase.

### *8.4.1. Phase Behavior*

Phase behavior of 74%Fluoroacrylate-26%Hexyl acrylate copolymer in $CO_2$ at ambient temperature is shown in Fig.1. Cloud point pressure of copolymer increases slightly with increasing polymer content in $CO_2$. The reason for dissolution of copolymer at reasonably low pressures might be due to electron donating functional group, i.e. carbonyl group, in the hexyl acrylate monomer as stated by several authors (7-9).

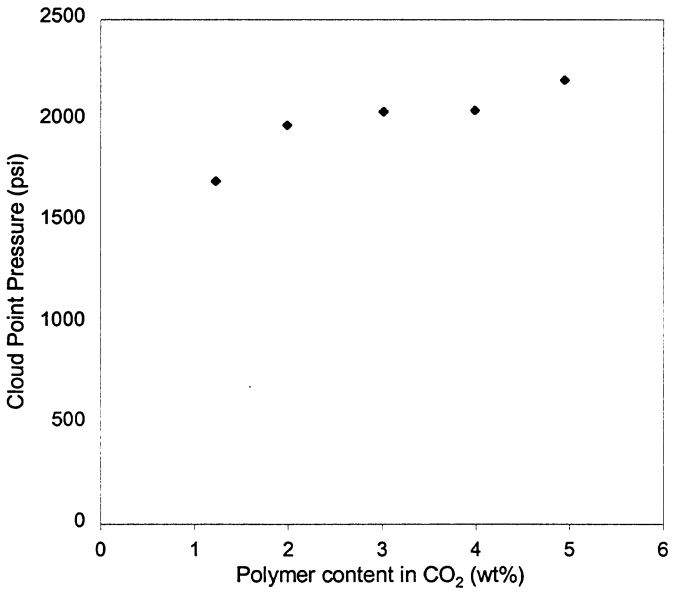


**Figure 1.** Phase behavior of 74%Fluoroacrylate-26%Hexyl acrylate copolymer in $CO_2$ at ambient temperature.

Seeing that copolymer dissolves easily in $CO_2$ despite of $CO_2$-phobic character of hexyl acrylate, 54%Fluoroacrylate-46%Hexyl acrylate copolymer was synthesized. However, with further increase in content of hexyl acrylate in copolymer, $CO_2$-phobic character of polymer dominated over attractive interactions between carbonyl group and carbon dioxide. At no concentrations of copolymer in $CO_2$, solubility of 54%Fluoroacrylate-46%Hexyl acrylate copolymer was observed.

Phase behavior of 16%Styrene-84%Fluoroacrylate copolymer is shown in Figure 2a. Despite of lack of acrylate group in the $CO_2$-phobic group, cloud point pressure did not exhibit tremendous change. Owing to random nature of the monomeric units in the copolymer, polymer dissolved in $CO_2$ rather forming micelle as happened in the case of block copolymer (3). Nakatani et al. studied effect of substituent on solubility of molecules in supercritical fluids (10). In their study they claimed that electron-releasing substituent increases relative solubility behavior of $CO_2$ while electron-withdrawing one decreases dissolution power of $CO_2$.

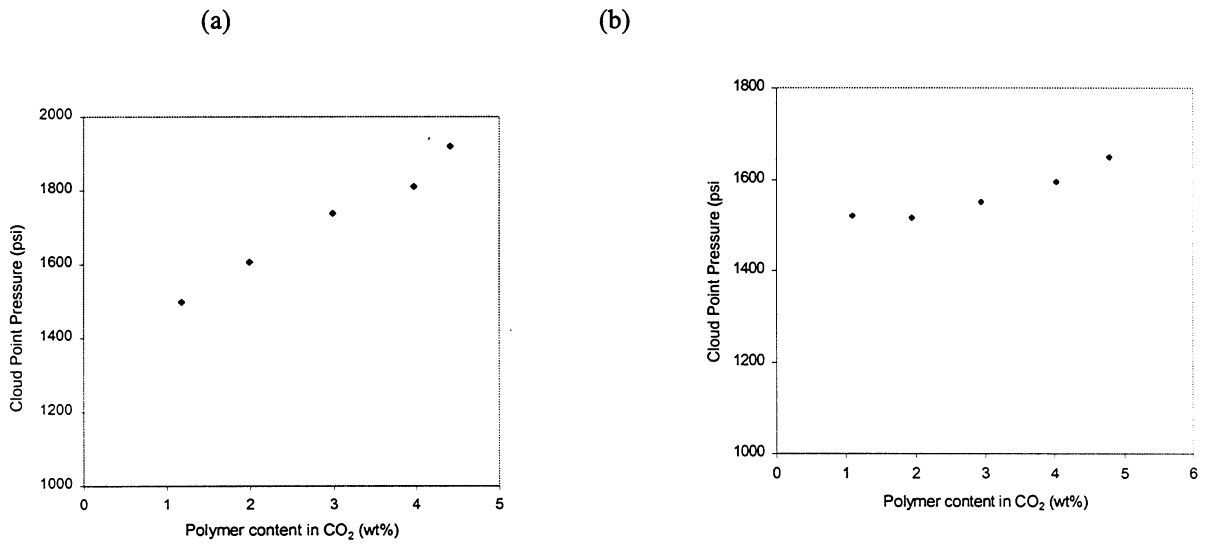


**Figure 2.** (a) Phase behavior of 84%Fluoroacrylate-16%Styrene copolymer in $CO_2$ at ambient temperature and (b) Phase behavior of 84%Fluoroacrylate-11%Styrene-5%Sulfonated Styrene copolymer in $CO_2$ at ambient temperature.

Holding this information in mind, we also observed that neutralized-sulfonated copolymer (84%Fluoroacrylate-11%Styrene-5%Sulfonated Styrene copolymer) solubilized relatively lower pressures at ambient temperature (Fig. 2b). We believe that this result happened due to $CO_2$ forming Lewis acid-base complexes with the polymer possessing negative ionic charge. However, we could not observe same solubility trend with the sample containing lower sulfonation degree, e.g. 84%Fluoroacrylate-14%Styrene-2%sulfonated styrene. At about 4.04 wt %, the polymer did not show any sign of solubility even at 5000 psi, but stayed as swollen network. After ventilation of $CO_2$, that swollen network fell out from the solution as very loose (98 % density

reduction), one-piece foam, filling the entire view cell. Foam structures of both samples were investigated via scanning electron microscopy (SEM). 84%Fluoroacrylate-11%Styrene-5%Sulfonated styrene copolymer was examined after $CO_2$ was vented out when the concentration was 1.05 wt %, and 84%Fluoroacrylate-14%Styrene-2%Sulfonated styrene copolymer at 4.04 wt %. In Fig. 3a and 3b, SEM image of both sulfonated polymers are shown at different magnification. As seen, foam is very flaky and contains a lot of voids in the sample with lower sulfonation degree. However the polymer containing higher level of sulfonation is more compact and the void fraction is lower. Still, why less sulfonated copolymer forms foam rather than dissolve is not clearly understood. But, this situation could be able to be explained by interference of intermolecular interactions, such as association of ionic group electron with $\pi$-electrons of aromatic group. If this suspicion is true, then interactions between $CO_2$ and ionic group in former one (more sulfonated one) dominate over interaction between ionic group and $\pi$-electrons of aromatic group.

To understand the effect of aromatic ring and substituent group on solubility, studies are currently concentrated on polymer molecules containing aromatic group in their structure. Being aware that acrylates are known electron donor, and electron pair on a acrylate carbonyl oxygen interacts with the carbon atom of $CO_2$ (7), we have proceeded our research synthesizing copolymer of fluoroacrylate with molecules possessing aromatic group as well as acrylate group. Fig. 4 illustrates phase behavior of 82%Fluoroacrylate-18%Phen ethyl acrylate copolymer. When Fig. 2a and Fig. 4 are compared, effect of acrylate group is revealed on solubility as such that cloud point pressures are lower.

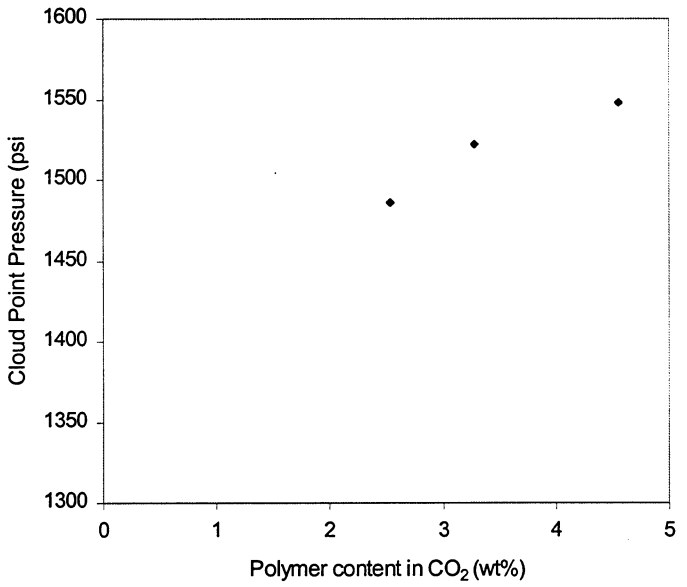


**Figure 4.** Phase behavior of 82%Fluoroacrylate-18%Phen ethyl acrylate copolymer in $CO_2$ at ambient temperature.

### *8.4.2. Viscosity Measurement*

In Figure 5, viscosity behavior of 74%Fluoroacrylate-26%Hexyl acrylate copolymer in $CO_2$ is illustrated. Relative viscosity of copolymer increases with increasing polymer concentration. As seen from the figure, ability of the copolymer to increase relative viscosity of solution at constant concentration increases with increasing pressure. However, pressure effect diminishes as the polymer concentration decreases.

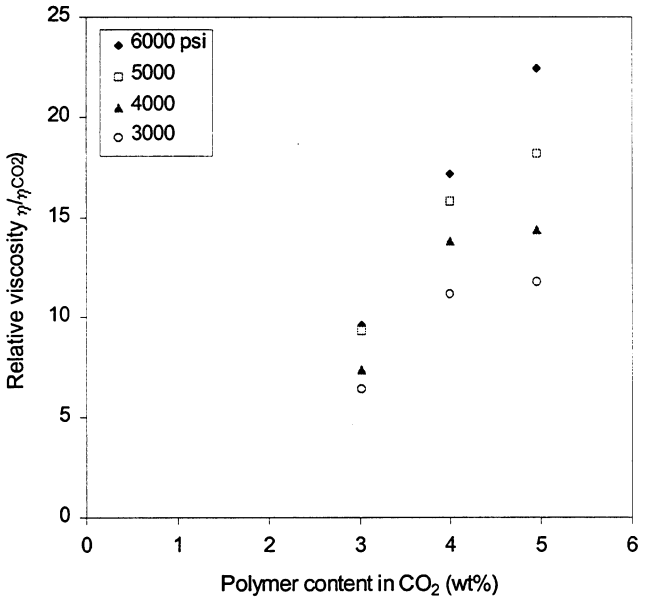


**Figure 5.** Relative viscosity of $CO_2$ solutions of 74%Fluoroacrylate-26%Hexyl acrylate Copolymer as a function of polymer content in $CO_2$.

Hexyl acrylate is linear molecule. Although it is soluble at reasonable pressures at ambient temperature, its effect on viscosity enhancement is not at desirable level. However the copolymer of fluoroacrylate with styrene shows a surprising increase in viscosity (Fig. 6). We surmise that stacking of aromatic groups causes this raise in viscosity. Stacking effect of aromatic moieties is pronounced more at high pressures. Surprisingly, sulfonation also contributed more to viscosity enhancement (Fig. 7). Seeing that aromatic group has an effect on viscosity improvement as well as dissolution power, now we directed our attention towards monomeric moieties containing aromatic ring in their structure. 82%Fluoroacrylate-18%Phen ethyl acrylate copolymer is the first example of the family (8). Different than Fluoroacrylate-Styrene Copolymer, Fluoroacrylate-Phen ethyl acrylate copolymer has two $CH_2$ spacer unit, and contains acrylate group which makes polymer easily dissolve in $CO_2$. Efforts are underway to complete the series (different combination of spacer units, aromatic rings) to better understand effect of aromatic units on solubility and viscosity.

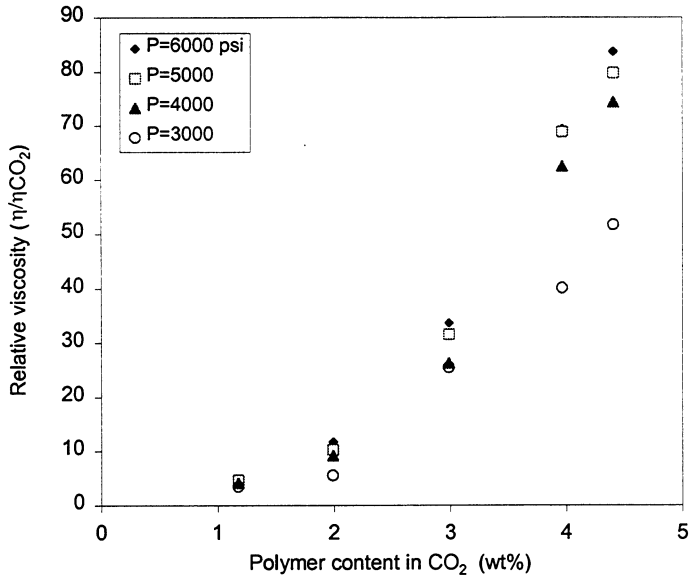


**Figure 6.** Relative viscosity of $CO_2$ solutions of 84%Fluoroacrylate-16%Styrene Copolymer as a function of polymer content in $CO_2$.

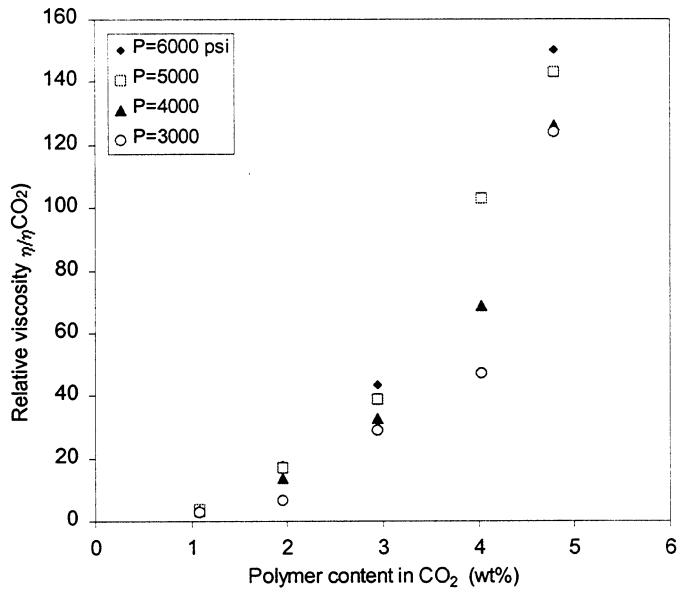


**Figure 7.** Relative viscosity of $CO_2$ solutions of 84%Fluoroacrylate-14%Styrene-5%Sulfonated Styrene Copolymer as a function of polymer content in $CO_2$.

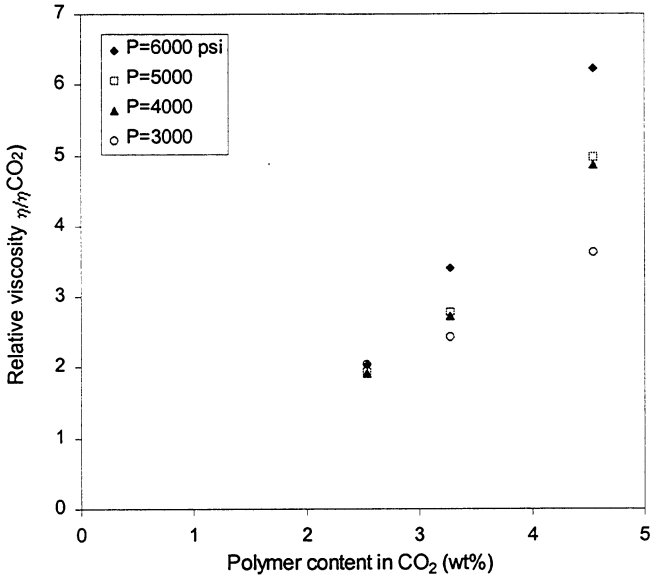


**Figure 8.** Relative viscosity of $CO_2$ solutions of 82%Fluoroacrylate-18%Phen ethyl acrylate copolymer as a function of polymer content in $CO_2$.

## 8.5 References


1. Shaffer, K. A., DeSimone, J. M., *Trends Polym. Sci.*, **3**, 146 (1995).
2. Fletcher, B., Suleman, N. K., Tanko, J. M., *J. Ame. Che. Soc.*, **120** (46), 11839 (1998).
3. Guan, Z., DeSimone, J. M., *Macromolecules*, **27**, 5527-5532 (1994).
4. Makowski; Henry S., Lundberg; Robert D., Singhal; Gopal H., US Patent 3,870,841.
5. Storey, R. F., Lee, Y., *J. Polym. Sci.: Part A: Poly. Chem.*, **31**, 31-44 (1993).
6. Orler, E. B., Yontz, D. J., Moore, R. B., *Macromolecules*, **26**, 5157-5160 (1993).
7. Eckert, C. A. and et. al, *J. Am. Chem. Soc.*, **118** (7), 1729 (1996).
8. McHugh, M. A., DiNoia, T. P., Rindfleisch, F., *J. Phys. Chem.*, **100**, 15581 (1996).
9. Eckert, C. A. and et. al, *J. Phys. Chem.*, **100**, 10837 (1996).
10. Nakatani, T., Ohgaki, K., Katayama, T., *Ind. Eng. Chem. Res.*, **30** (6), 1362 (1991).

## Appendix. Falling Cylinder Viscometry Study

### 1. Introduction to Detailed Study of Solution Viscosity Using Falling Cylinder Viscometry

In this section of the annual report, we show how one can design molecules that are both highly $CO_2$-soluble and which aggregate in solution. When associating polymers are employed, we have observed the 2 order of magnitude increase in viscosity, as determined by falling cylinder viscometry. The shear rate- and concentration-dependence of the solution viscosity are reported.

## 2. Experimental Procedure

Polymer Synthesis

*Heptadecafluorodecylacrylate-Styrene Copolymer*

Bulk polymerized 79%heptadecafluorodecyl acrylate - 21% styrene random copolymers are the most promising carbon dioxide thickeners identified to date. They can increase the viscosity of carbon dioxide by a factor of 250 at a concentration of 5wt%. We postulate that

a. bulk polymerization leads to higher copolymer molecular weight
b. the fluoroacrylate monomer enables the copolymer to dissolve in carbon dioxide
c. the styrene monomer leads to macromolecular formation via pi-pi stacking, but also causes the copolymer to become less carbon dioxide-soluble
d. increasing the fraction of styrene in the copolymer from 0-29% results in the *intermolecular* "stacking" of aromatic rings (associated with the styrene monomer), leading to viscosity-enhancing macromolecular formation in $CO_2$ solutions
e. increasing the fraction of styrene beyond 29% leads to the polymer coiling upon itself (because it is becoming more carbon dioxide-phobic) and *less effective* viscosity-enhancing *intramolecular* associations of the aromatic groups

Because the heptadecafluorodecyl acrylate monomer is very expensive and not available in bulk volume, several commercial grade fluorinated acrylate monomers were considered.

*Perfluoroalkylethacrylate-Styrene Copolymers*

Asahi Glass FA-X monomer is a relatively inexpensive commercially available polydisperse perfluoroalkyl ethyl acrylate monomer. The carbon chain length of the fluorinated tail is 6-16, 2-perfluoroalkyl(C6-C16)ethyl acrylate. Because the structure of the perfluoroalkyl ethyl acrylate monomer is similar to the heptadecafluorodecyl acrylate, we examined the possibility of generating FA-X – styrene copolymers for $CO_2$-thickening. The synthesis of FA-x homopolymer is similar to the synthesis of copolymer. FA-X alone was employed as the monomer, however.

We synthesized both the homopolymer of FA-X and random copolymers of FA-X and styrene. The following steps were employed during the synthesis of the random copolymers.

1. Purify the FA-X: Wash FA-X with 5% NaOH three times, wash it with distilled water three times, add $MgSO_4$ to remove trace water, put it into refrigerator, filter it to get purified FA-X.
2. Use AIBN as initiator, put 0.2% (mol) of AIBN into ample.

3. Add specific amount of distilled styrene.
4. Add specific amount of purified FA-x into ample.
5. Send $N_2$ into ample to remove $O_2$, seal the ample.
6. Put the ample in silicon oil (60° C), overnight.
7. Use Freon 113 to dissolve the copolymer, and wash the copolymer with methyl alcohol several times.

The carbon dioxide solubility results of the perfluoroalkyl ethyl acrylate – styrene copolymers and the perfluoroalkyl ethyl acrylate homopolymer were not promising. We were unable to dissolve either in dense carbon dioxide. *Therefore we will not use fluoroalkyl ethyl acrylate (or fluoroalkyl methyl acrylate) monomers in any future thickening agents.* The presence of the small alkyl group (methyl or ethyl) on the fluoroalkyl acrylate monomer leads to substantial decreases in carbon dioxide solubility of polymers.

*Fluoroalkyl Acrylate-Styrene Copolymers*

3M and Elf Atochem produce commercial amounts of a fluoroalkyl acrylate for the manufacture of fluoroacrylate copolymers. We have contacted both companies and are attempting to obtain samples of their fluoroalkyl acrylate monomers.

Falling Cylinder Viscometry

Based on our previous findings, the 29%styrene-71%fluoroacrylate copolymer showed the greatest promise. Therefore we conducted a thorough falling cylinder viscometry assessment of its carbon dioxide thickening potential. The copolymer was $CO_2$ soluble, and the mixture of copolymer and $CO_2$ was transparent. We have previously presented the details of the solubility of the polymer in carbon dioxide.

Falling cylinder viscometry [14-16] was conducted by observing the terminal velocity of an aluminum cylinder falling through neat carbon dioxide or a single phase, transparent solution of carbon dioxide and the copolymer. The ratio of the terminal velocities (velocity in neat carbon dioxide/velocity in thickened carbon dioxide) was directly proportional to the increase in viscosity. Each terminal velocity experiment was repeated 5-7 times.

The major characteristics of the high pressure falling cylinder viscometer are summarized in the following table.

| | |
|---|---|
| Cylinder material | Aluminum |
| Cylinder specific gravity | 2.7 |
| Cylinder length | 0.8268 in |
| Cylinder #1 diameter | 1.2450 in |
| Cylinder #2 diameter | 1.2438 in |
| Cylinder #3 diameter | 1.2428 in |
| Cylinder #4 diameter | 1.2399 in |
| Cylinder #5 diameter | 1.2339 in |
| Cylinder #6 diameter | 1.2311 in |
| Cylinder #7 diameter | 1.2293 in |
| Cylinder #8 diameter | 1.2269 in |
| Quartz hollow cylinder ID | 1.2500 in |
| Distance travelled by falling cylinder | 5-12 cm |
| Fluid | Neat $CO_2$ or thickened $CO_2$ |

Table 1. Characteristics of the Falling Cylinder Viscometer

## 3. **Viscometer Calibration Constants and Example Calculations**

*Theoretical and experimental calibration constants*

From derivation, we assume the $CO_2$ solution is Newtonian fluid, so,

$$\mu = K\frac{\rho_c - \rho_f}{Vc}$$

Then, we can compare the experimental calibration constant K with the theoretical calibration constant, ignoring the resistances because non-ideal falling.

In our falling cylinder viscometer, we use pure $CO_2$ as our sample, at specific temperature (297K), and specific pressure (3000psi), we can get experimental calibration constant:

$$K = \frac{\mu\, Vc}{\rho_c - \rho_f}$$

We can also get theoretical calibration constant from the size of the falling cylinder:

$$K = \frac{r_c g}{r_c J' - 2K'}$$

Where,

$$J' = -\frac{4}{(r_t^2 - r_c^2) + \ln\frac{r_c}{r_t}(r_t^2 + r_c^2)}$$

$$K' = \frac{-2r_c - (r_t^2 - r_c^2)\dfrac{1}{r_c \ln(r_c/r_t)}}{r_t^2 - r_c^2 + \ln(r_c/r_t)(r_t^2 + r_c^2)} + \frac{1}{r_c \ln(r_c/r_t)}$$

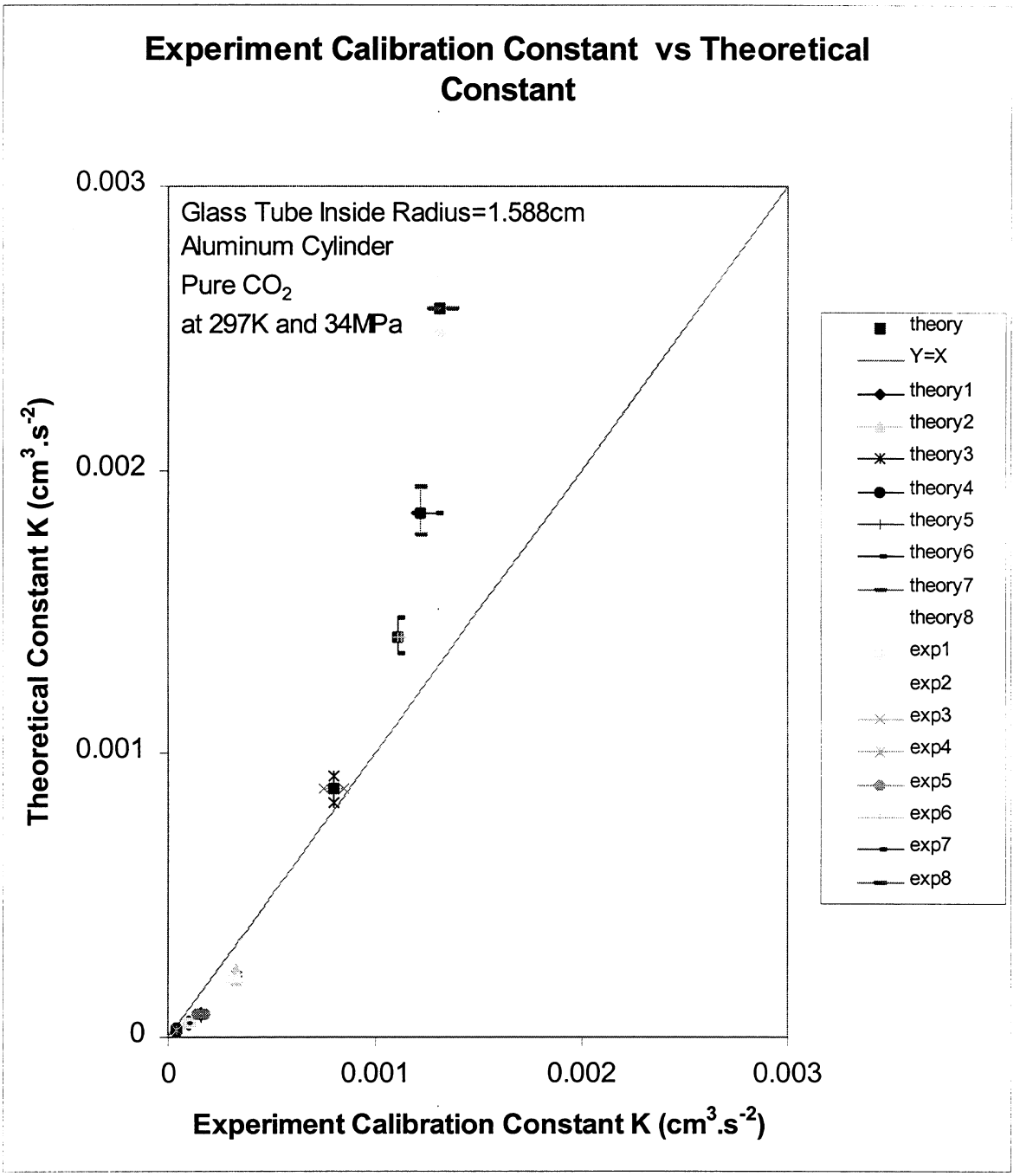


The diagonal line corresponds to an exact agreement between the predicted and actual calibration constant for the viscometer. The agreement is quite reasonable for the cylinders with a low calibration constant (slowly falling, larger diameter, closer clearance aluminum cylinders with a small annular gap between the falling cylinder and the inner

surface of the quartz tube). For the smaller diameter cylinders, the cylinders fall at a slower rate than expected from theory. This can be attributed to the unstable nature of the fall, as evidenced by these cylinders not falling coaxially through the fluid within the quartz cylinder. One can observe the cylinder wobbling and contacting the quartz cylinder during when these cylinders are employed. Despite this disagreement between the theoretical and experimental values of the calibration constant, the device can still be used to provide an accurate, but not precise, indication of whether substantial increases in carbon dioxide viscosity are occurring.

The vertical line segment is theoretical constant "error bar", because of the variations of the OD of the aluminum cylinder (±0.00015 inch). The horizontal error bar provides an indication of the variance of the 5-7 readings obtained for the terminal velocity.

## 4. Results and Discussion

The viscosity results are summarized in the following figure. The viscosity of $CO_2$ is enhanced 250-fold in 5wt% copolymer-$CO_2$ solution, and even in 1wt% solution, the viscosity of $CO_2$ was increased several times. In lower concentration, 0.2wt%, 0.1wt%, there is a discernible viscosity increase. The shear rate and relative viscosity ranges of interest to this project are illustrated by the rectangle in this figure. Although we were not able to obtain data in this region using our falling cylinder viscometer, the extrapolation of the 1.0 and 0.2 wt% results indicate that it may be possible to attain the desired degree of thickening using very dilute concentrations of the polymer.

When viscosity is determined next year using pressure drops for solutions flowing through porous media [17], dilute concentrations (0.1-0.2 wt%) of this copolymer will be employed during the initial tests.

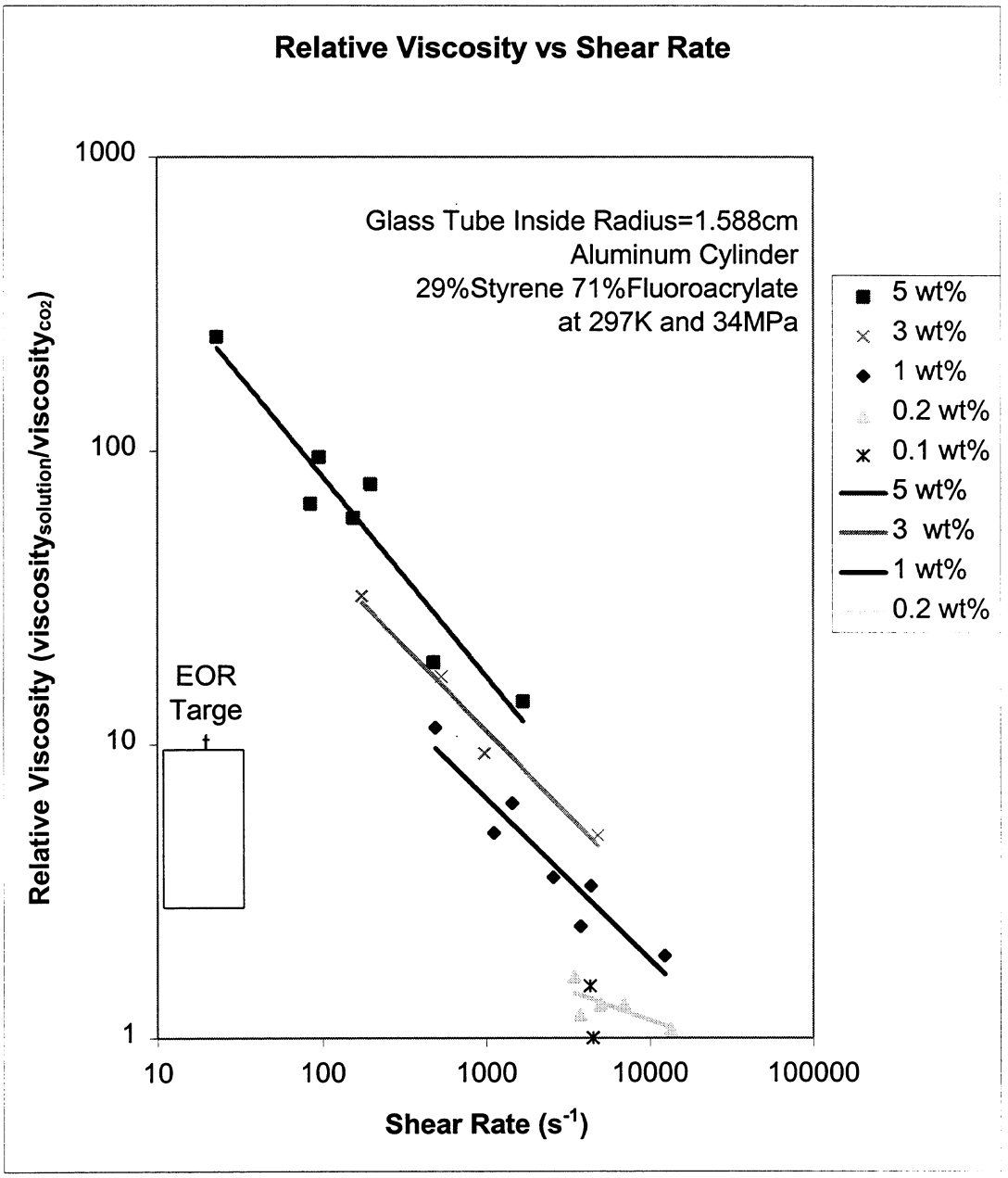
Relative Viscosity vs Shear Rate
Glass Tube Inside Radius=1.588cm
Aluminum Cylinder
29%Styrene 71%Fluoroacrylate
at 297K and 34MPa
EOR
Targe
t
5 wt%
3 wt%
1 wt%
0.2 wt%
0.1 wt%
5 wt%
3 wt%
1 wt%
0.2 wt%
1000
100
10
1
10
100
1000
10000
100000
Relative Viscosity (viscosity$_{solution}$/viscosity$_{CO2}$)
Shear Rate (s$^{-1}$)

## 5. References


1. J.M. DeSimone, Z. Guan, C.S. Elsbernd, Science (1992), 257, 945

2. C. Lepilleur, E.J. Beckman, Macromolecules (1997), 30, 745

3. O'Neill, M.L.; Yates, M.Z.; Harrison, K.L.; Johnston, K.P.; Canelas, D.A.; Betts, D.E.; DeSimone, J.M.; Wilkinson, S.P.; Macromolecules (1997), 30, 5050

4. P.G. Jessop, T. Ikariya, R. Noyori, Chem. Rev. (1999), 99, 475

5. (a) D. Hancu, E.J. Beckman, Industr. Eng. Chem. Res. (1999), 38, 2824 (b) D. Hancu, E.J. Beckman, Industr. Eng. Chem. Res. (1999), 38, 2833

6. A.J. Mesiano, E.J. Beckman, A.J. Russell, Chem. Rev. (1999), 99 623

7. M. Super, E.J. Beckman, Trends in Polym. Sci. (1997), 5, 236

8. D.J. Darensbourg, M.W. Holtcamp, Coord. Chem. Rev. (1996), 153, 155

9. Fulton, J.L.; Pfund, D.M.; McClain, J.B.; Romack, T.J.; Maury, E.E.; Combes, J.R.; Samulski, E.T.; DeSimone, J.M.; Capel, M.; Langmuir (1995), 11, 4241

10. F.I. Stalkup, "Miscible Displacement", SPE Monograph No 8., New York, NY (1983)

11. D.K. Dandge, J. Heller, C. Lien, K.J. Wilson; J. Appl. Polym. Sci. (1986), 32, 5373

12. P. Gullapalli, J-S. Tsau, J.P. Heller, SPE Int. Symp. On Oilfield Chem., paper SPE 28979, Houston, TX, Feb., 1995

13. R.M. Enick, A. Iezzi, P. Bendale, J. Brady, Fluid Ph. Equil. (1989), 53, Part II, 307; C.A. Irani, T.V. Harris, W.R. Pretzer, U.S. patents 4,945,990 (1990); also U.S. patent 4.945,989 (1990)

14. Eichstadt, F. J., Swift, G. W.,"Theoretical Analysis of the Falling Cylinder Viscometer for Power Law and Bingham Plastic Fluids", A.I.Ch.E Journal, V. 12, No. 6 (1966), p1179

15. Lohrenz J., Kurata, F., "Design and Evaluation of a New Body for Falling CylinderViscometers", A.I.Ch.E Journal, V. 8, No. 2 (1962) p190

16. Lohrenz J., Swift, G. W., Kurata, F., "An Experimental Verified Theoretical Study of the Falling Cylinder Viscometer", A.I.Ch.E Journal, Vol 6, No.4 (1960) p547

17. Bae, J. H., Irani, C. A., "A Laboratory Investigation of Thickened CO2 Process", paper SPE 20467 p73, 1990, 65th Annual Technical Conference and Exhibition of SPE, New Orleans, LA, Sept. 23-26, 1990.